Gravity-induced photon interactions and infrared consistency in any dimensions

Pedro Bittar[®], ^{1,*} Sylvain Fichet[®], ^{2,†} and Lucas de Souza[®], ^{3,‡}

¹Department of Mathematical Physics, University of São Paulo, São Paulo, 05508-090 SP, Brazil ²CCNH, Federal University of ABC, Santo André, 09210-580 SP, Brazil ³CMCC, Federal University of ABC, Santo André, 09210-580 SP, Brazil

(Received 12 November 2024; accepted 18 July 2025; published 21 August 2025)

We compute the four-photon (F^4) operators generated by loops of charged particles of spin $0, \frac{1}{2}, 1$ in the presence of gravity and in any spacetime dimension d. To this end, we expand the one-loop effective action via the heat kernel coefficients, which capture both the gravity-induced renormalization of the F^4 operators and the low-energy Einstein-Maxwell effective field theory (EFT) produced by massive charged particles. We set positivity bounds on the F^4 operators using standard arguments from extremal black holes (for $d \ge 4$) and from infrared (IR) consistency of four-photon scattering (for $d \ge 3$). We find that both approaches yield nearly equivalent results, even though in the amplitudes we discard the graviton t-channel pole and use the vanishing of the Gauss-Bonnet term at quadratic order for any d. The positivity bounds constrain the charge-to-mass ratio of the heavy particles. If the Planckian F^4 operators are sufficiently small or negative, such bounds produce a version of the d-dimensional weak gravity conjecture (WGC) in most, but not all, dimensions. In the special case of d = 6, the gravity-induced beta functions of F^4 operators from charged particles of any spin are positive, leading to WGC-like bounds with a logarithmic enhancement. In d = 9, 10, the WGC fails to guarantee extremal black hole decay in the infrared EFT, thereby requiring the existence of sufficiently large Planckian F^4 operators.

DOI: 10.1103/p8k8-vz2h

I. INTRODUCTION

In the quest to unravel the mysteries of quantum gravity, one route involves a thorough examination of gravitational effective field theories (EFTs) that appear below the Planck scale. Such gravitational EFTs are constrained by black hole physics and, like non-gravitational ones, by infrared consistency conditions based on unitarity and causality. In the presence of gravity, ultraviolet (UV) and infrared (IR) scales seem to feature intricate connections, already at the classical level as hinted by black hole properties. This implies that, even though the completion of quantum gravity lies far in the UV, we can hope to gain insights by scrutinizing gravitational EFTs in the IR.

The notion of IR consistency of EFTs, that implies bounds on certain Wilson coefficients, has been introduced in [1–3]. It has led to many subsequent developments;

Contact author: pedro.bittar.souza@usp.br Contact author: sylvain.fichet@ufabc.edu.br *Contact author: souza.l@ufabc.edu.br

Published by the American Physical Society under the terms of the Creative Commons Attribution 4.0 International license. Further distribution of this work must maintain attribution to the author(s) and the published article's title, journal citation, and DOI. Funded by SCOAP³.

see, e.g., [4-26]. Black hole physics is also used to put bounds on gravitational EFTs [27–35]. The consistency of EFTs with the UV completion of quantum gravity has been explored via "swampland" conjectures; see, e.g., the first weak gravity conjecture [36] and recent reviews [37–39]. Conversely, the IR consistency of gravitational EFTs constrains UV completions of quantum gravity and thus has an interplay with swampland conjectures [26,33,40–46]. The present work is in the spirit of the latter approach: carving out the space of gravitational EFTs from the IR, using consistency conditions from both scattering amplitudes and black holes.

Our focus in this work is on gravitational EFTs that feature an Abelian gauge symmetry. We refer to the Abelian gauge field as the photon. We consider an EFT arising below the Planck scale $M_P \equiv M$, the *ultraviolet* EFT, that features a charged particle. We consider charged particles with spin $0, \frac{1}{2}, 1$ and arbitrary spacetime dimensions d.

The sub-Planckian EFT features, in general, local fourphoton operators that we denote here collectively as F^4 . The F^4 coefficient α_{UV} encapsulates the sub-Planckian effects from the super-Planckian UV completion. Depending on the spacetime dimension, loops of charged particles may renormalize the F^4 operators, in which case the value α_{UV} is understood as the value of the coefficient at the Planck scale. As a first step, we will compute at one-loop this F^4 renormalization flow, that occurs regardless of whether the particle is massless or massive.

Additionally, when the charged particle is massive, it can be integrated out when the renormalization scale is much lower than the particle mass. This produces another *infrared* EFT whose only degrees of freedom are the photon and the graviton. EFTs of this kind are usually referred to as Einstein-Maxwell theory; here we mostly use the term IR EFT. The IR EFT contains a F^4 operator with coefficient

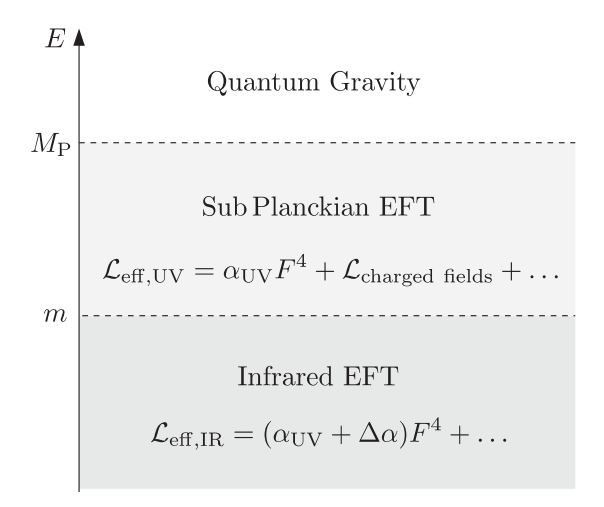
$$\alpha_{\rm IR} = \alpha_{\rm UV} + \Delta \alpha,$$
 (1.1)

where the $\Delta \alpha$ corrections take schematically the form

$$\Delta \alpha = a \frac{g^4 q^4}{m^{8-d}} + b \frac{g^2 q^2}{m^{6-d} M^{d-2}} + \frac{c}{m^{4-d} M^{2d-4}}, \qquad (1.2)$$

where m is the charged particle mass. In certain dimensions, some of the coefficients are enhanced by $\log(\frac{M}{m})$ terms produced by the renormalization flow.

The various scales and EFTs are summarized as follows:



Our approach in this work is to remain fully agnostic about the UV completion of quantum gravity. We work with quantum field theory—and do not perform actual quantum gravity calculations. The only explicit matching to a specific string theory is given in Appendix A as an example. The strength of the EFT approach is that our ignorance of the UV completion of quantum gravity is encoded into the values of the $\alpha_{\rm UV}$ coefficients, which are treated here as free parameters.

We perform the computation of both the F^4 one-loop beta functions and of the IR EFT directly from the one-loop effective action. We use the background field method and the heat kernel formalism [see [47–49]; other useful references are [50–54]] combined with standard EFT techniques.

The sequence of EFTs can be used to compute the contribution of the charged particle to the physical process of four-photon scattering $\gamma\gamma \to \gamma\gamma$ at low energy. Such a process is subject to IR consistency bounds from unitarity and causality. In an appropriate basis, IR consistency implies positivity of the F^4 coefficients, schematically ¹

$$\alpha_{\rm IR} \ge 0. \tag{1.3}$$

The IR EFT can also be used to compute the metric of nonrotating charged black holes with large enough radius [55,56]. Requiring that such extremal black holes be able to decay produces a positivity bound similar to (1.3).²

Combining the positivity bound (1.3) with Eqs. (1.1) and (1.2), one can notice that, for appropriate values and signs of $\alpha_{\rm UV}$, a, b, c, a lower bound appears on the charge-to-mass ratio,

$$\frac{g|q|}{m}M^{\frac{d-2}{2}} \equiv z \ge z_*,\tag{1.4}$$

with z_* being a dimensionless number dependent on $\alpha_{\rm UV}$, a, b, c. Equation (1.4) is precisely the parametric form of the weak gravity conjecture (WGC) in d-dimensions [see [57]], in which case the bound is $z_* = \sqrt{\frac{d-3}{d-2}}$. For z_* being a generic O(1) coefficient, we refer to bounds of the form (1.4) as WGC-like. This nontrivial connection between IR and UV consistency was first pointed out in [40] for d=3, 4. Because the pattern of signs and divergences of the a, b, c coefficients is dimension-dependent, the generalization of this phenomenon to arbitrary d is nontrivial and requires a thorough investigation. Here we explore the IR consistency/WGC connection in arbitrary dimension and revisit the d=3, 4 cases.

Why might one study arbitrary spacetime dimensions in the first place? While the known real world displays d=3+1 dimensions, it is plausible that extra dimensions exist—in particular, string theory requires d=11 for consistency. These dimensions may be hidden from us, either because they are compact or because our matter is confined to a three-brane within a higher-dimensional bulk spacetime. More specifically, in this work, we extend to higher dimensions as a tool to probe the relations among several concepts: the WGC, the decay of extremal black holes (see Sec. III A), and the IR consistency of scattering amplitudes. We investigate, for any $d \ge 4$, the extent to

¹For simplicity, we use the most basic positivity bound from [3], that we extend to higher dimensions. More refined approaches have been developed; see, e.g., [4–24], that are not the focus of this work.

²The extremal black hole decay condition is sometimes referred to as the *black hole* WGC. Here we do not use this naming; the term WGC only refers to the condition on the charged particle, (1.4).

which the WGC implies the decay of extremal black holes of any size, and whether IR consistency implies extremal black hole decay and the WGC. In our approach, testing whether a relation between two concepts holds for any d serves as a check of its robustness. We take the viewpoint that, if a given relation qualitatively changes with spacetime dimension, it is unlikely to reflect a deep physical principle, and should instead regarded as coincidental. In sum, the extension to arbitrary d provides a diagnostic for sharpening and validating our understanding of gravity in d=4.

A. Outline

In Sec. II, we review EFT beyond tree-level from the viewpoint of the quantum effective action. We define the Einstein-Maxwell EFT and show how to reduce it using a property of the Gauss Bonnet term valid in any dimensions. In Sec. III, we review the bound from extremal black hole decay and generalize simple positivity bounds from fourphoton scattering to any dimension. In Sec. IV, after reviewing the heat kernel coefficients, we derive and reduce the general one-loop effective action obtained from integrating out charged particles of spin 0, $\frac{1}{2}$ and 1. In Sec. V, we present the F^4 beta functions and discuss their interplay with IR consistency. In Sec. VI, we analyze in detail the IR consistency of the infrared EFT, with a systematic discussion from d = 3 to 11. Section VII contains a detailed summary, and the appendixes contains some examples of UV realizations of the F^4 operators (Appendix A), the detailed analysis of the bound from infrared consistency (Appendix B) and extremal black hole decay (Appendix C), and the complete heat kernel coefficients (Appendix D).

II. EINSTEIN-MAXWELL EFT IN ANY DIMENSIONS

We briefly review the notion of loop-level low-energy EFT from the viewpoint of the quantum effective action in Sec. II A. We then define Einstein-Maxwell EFT in Sec. II B and show how to reduce it to describe photon scattering in Secs. II C and II D.

A. Effective action and effective field theory

Consider a theory with light fields Φ_{ℓ} and heavy fields Φ_h . Assume that our interest lies in the scattering amplitudes of the light fields. Such scattering amplitudes are obtained by taking functional derivatives of the generating functional of connected correlators with respect to sources probing the light fields J_{ℓ} . This generating functional is $W[J_{\ell}] = i \log Z[J_{\ell}]$ with the partition function

$$Z[J_{\ell}] = \int \mathcal{D}\Phi_{\ell} \mathcal{D}\Phi_{h} e^{iS[\Phi_{\ell},\Phi_{h}]+i\int d^{d}x \Phi_{\ell} J_{\ell}}.$$
 (2.1)

We perform the Φ_h field integral in the partition function. This defines a "partial" quantum effective action $\Gamma_h[\Phi_\ell]$,

with

$$Z[J_{\ell}] = \int \mathcal{D}\Phi_{\ell} e^{i\Gamma_h[\Phi_{\ell}] + i \int dx^d \Phi_{\ell} J_{\ell}}.$$
 (2.2)

Let us consider the low-energy regime for which the external momenta of the Φ_ℓ amplitudes are much smaller than the mass of the heavy fields, noted m. In this limit, the quantum effective action Γ_h can be organized as an expansion in powers of derivatives over m. This is conveniently expressed as an effective Lagrangian \mathcal{L}_{eff}

$$\Gamma_h[\Phi_\ell] \equiv \int d^d x \sqrt{-g} \mathcal{L}_{\text{eff}}[\Phi_\ell],$$
 (2.3)

where \mathcal{L}_{eff} is made of monomials of Φ_{ℓ} and its derivatives, suppressed by powers of m. Schematically,

$$\mathcal{L}_{\text{eff}}[\Phi_{\ell}] \sim \sum_{a,b} \frac{\Phi_{\ell}^{a} (\partial \Phi_{\ell})^{2b}}{m^{a+4b-4}}.$$
 (2.4)

In practice, \mathcal{L}_{eff} is typically truncated at some order of the derivative expansion ∂/m . This defines an infrared EFT that encodes all the effects of the Φ_h field at energies below m, within the accuracy of the truncation of \mathcal{L}_{eff} .

The derivative expansion applies at each order of the loop expansion of Γ_h , $\Gamma_h = \Gamma_h^{(0)} + \Gamma_h^{(1)} + \cdots$ Hence, the effective Lagrangian can be organized with respect to this loop expansion: $\mathcal{L}_{\text{eff}} = \mathcal{L}_{\text{eff}}^{(0)} + \mathcal{L}_{\text{eff}}^{(1)} + \cdots$ The $\mathcal{L}_{\text{eff}}^{(0)}$ term arises from the tree diagrams involving Φ_h encoded in $\Gamma_h^{(0)}$. The $\mathcal{L}_{\text{eff}}^{(1)}$ term arises from the one-loop diagrams involving Φ_h encoded in $\Gamma_h^{(1)}$, etc.

In this paper, we work at the one-loop level. The finer details of EFT at loop level can be found in [58,59].

B. Einstein-Maxwell EFT

Consider a gravitational theory with a U(1) gauge symmetry and massive matter fields.³ Our interest is in the scattering amplitudes of the photons of this theory; i.e., the photon is coupled to a source J_{γ} that generates the amplitudes. As explained in Sec. II A, we can always integrate out the matter fields exactly, defining a partial quantum effective action $\Gamma_{\text{mat}}[F_{\mu\nu}, R_{\mu\nu\rho\sigma}]$.

In the regime for which the external momenta of amplitudes are smaller than the matter field masses m, the quantum effective action can be written as

 $^{^3}$ Throughout this work we use the conventions of Misner-Thorne-Wheeler [60], which include the mostly plus metric signature $\mathrm{sgn}(g_{\mu\nu})=(-,+,\cdots,+)$ and positive scalar curvature for spheres.

$$\Gamma_{\text{mat}}[F_{\mu\nu}, R_{\mu\nu\rho\sigma}] \equiv \int d^d x \sqrt{-g} \mathcal{L}_{\text{eff}}[F_{\mu\nu}, R_{\mu\nu\rho\sigma}], \qquad (2.5)$$

where \mathcal{L}_{eff} is made of monomials of $F_{\mu\nu}$ and $R_{\mu\nu\rho\sigma}$. This defines a low-energy EFT that encodes all the effects of the matter fields at energies below m. In this section, we refer to this EFT as the Einstein-Maxwell EFT, with $\mathcal{L}_{\text{eff}} \equiv \mathcal{L}_{\text{EM}}$. At ∂^4 order, the most general Einstein-Maxwell Lagrangian takes the form⁴

$$\mathcal{L}_{\rm EM} = \mathcal{L}_{\rm kin} + \alpha_1 (F^{\mu\nu} F_{\mu\nu})^2 + \alpha_2 F^{\mu\nu} F_{\nu\rho} F^{\rho\sigma} F_{\sigma\mu} + \alpha_3 \hat{R}^2 + \alpha_4 \hat{R}_{\mu\nu} \hat{R}^{\mu\nu} + \alpha_5 \hat{R}_{\mu\nu\rho\sigma} \hat{R}^{\mu\nu\rho\sigma} + \alpha_6 \hat{R} F^{\mu\nu} F_{\mu\nu} + \alpha_7 \hat{R}^{\nu}_{\mu} F^{\mu\rho} F_{\nu\rho} + \alpha_8 \hat{R}^{\rho\sigma}_{\mu\nu} F^{\mu\nu} F_{\rho\sigma} + \alpha_9 (D_{\rho} F_{\mu\nu}) (D^{\rho} F^{\mu\nu}) + \alpha_{10} (D_{\rho} F_{\mu\nu}) (D^{\mu} F^{\rho\nu}) + \alpha_{11} (D^{\mu} F_{\mu\nu})^2 + O(\hat{R}^3, \hat{R}^2 F^2, \hat{R} F^4, F^6)$$
(2.6)

with the kinetic term

$$\mathcal{L}_{kin} = -\frac{1}{4}F_{\mu\nu}F^{\mu\nu} + \frac{1}{2}\hat{R}.$$
 (2.7)

We introduced the normalized Riemann tensor $\hat{R}_{\mu\nu\rho\sigma} \equiv M^{d-2} R_{\mu\nu\rho\sigma}$.

At tree-level, the effective operators in \mathcal{L}_{EM} contribute to the four-photon amplitude as follows:

The dots represent the effective vertices from \mathcal{L}_{EM} , and the double wiggles represent gravitons. Notice that the curvature operators contribute indirectly via modifications of the graviton-photon vertices and to the graviton propagator.

These diagrams can be simplified using that the physical scattering amplitudes are invariant under field redefinitions. Following the general lessons of EFT, a subset of such field redefinitions amounts to using the leading order equations of motion in the effective Lagrangian [59]. In the present case, the equations of motion that we can use are the Maxwell and Einstein equations: $D^{\mu}F_{\mu\nu}=0$ and $R_{\mu\nu}-\frac{1}{2}Rg_{\mu\nu}=\frac{1}{M^{d-2}}T_{\mu\nu}$. The latter implies

$$\hat{R}_{\mu\nu} = T_{\mu\nu} - \frac{1}{d-2} T g_{\mu\nu}, \qquad \hat{R} = \frac{2}{2-d} T$$
 (2.9)

with

$$T_{\mu\nu} = -F_{\mu\rho}F^{\rho}_{\nu} - \frac{1}{4}g_{\mu\nu}(F_{\rho\sigma})^2, \qquad T = \frac{4-d}{4}(F_{\mu\nu})^2.$$
 (2.10)

Using the Maxwell equation, the last operator in \mathcal{L}_{EM} vanishes. Furthermore, the two other operators involving $D_{\mu}F_{\rho\sigma}$ can be transformed into combinations of the remaining terms in \mathcal{L}_{EM} using the Bianchi identities

 $F_{[\mu\nu;\rho]}=0$, $R_{\mu[\nu\rho\sigma]}=0$, and the Ricci identity $[D_{\mu},D_{\nu}]F_{\rho\sigma}=R^{\lambda}_{\mu\nu\rho}F_{\lambda\sigma}+R^{\lambda}_{\mu\nu\sigma}F_{\rho\lambda}.^{5}$ Finally, the identities from (2.9) can be used to eliminate R and $R_{\mu\nu}$ in the remaining operators of $\mathcal{L}_{\rm EM}$. The traceless part of the Riemann tensor, i.e., the Weyl tensor,

$$C_{\mu\nu\rho\sigma} = R_{\mu\nu\rho\sigma} - \frac{2}{d-2} (g_{\mu[\rho} R_{\sigma]\nu} - g_{\nu[\rho} R_{\sigma]\mu}) + \frac{2}{(d-1)(d-2)} R g_{\mu[\rho} g_{\sigma]\nu}, \qquad (2.12)$$

still remains in \mathcal{L}_{EM} in the form of operators C^2 and CF^2 .

C. Reducing the curvature squared terms

We can further reduce the basis of operators by noticing that, for the four-photon diagrams of our interest, the graviton self-interactions are irrelevant since only the graviton propagator appears in (2.8). Let us inspect the quadratic curvature corrections to the graviton propagator.

We know that the Riemann tensor goes as $R_{\mu\nu\rho\sigma} \propto \partial_{\mu}\partial_{\sigma}h_{\nu\rho} + \cdots$ upon the expansion of the metric $g_{\mu\nu} = \eta_{\mu\nu} + h_{\mu\nu}$. It is thus sufficient to keep the linear term in

$$\begin{split} D_{\rho}F_{\mu\nu}D^{\rho}F^{\mu\nu} &= R_{\mu\nu\rho\sigma}F^{\mu\nu}F^{\rho\sigma} - 2R^{\nu}_{\mu}F^{\mu\rho}F_{\nu\rho} + 2(D^{\mu}F_{\mu\nu})^2 \\ &\quad + \text{total derivative}. \end{split} \tag{2.11}$$

⁴We assume a spacetime background with no boundary, so that total derivative terms in \mathcal{L}_{EM} can be ignored, and operators related by integration by parts are considered redundant.

⁵For example, one finds

each curvature term to obtain the quadratic vertices that correct the graviton propagator. We have

$$R_{\mu\nu\rho\sigma} = \frac{1}{2} \left(\partial_{\mu} \partial_{\sigma} h_{\nu\rho} - \partial_{\nu} \partial_{\sigma} h_{\mu\rho} - \partial_{\mu} \partial_{\rho} h_{\nu\sigma} + \partial_{\nu} \partial_{\rho} h_{\mu\sigma} \right) + O(h^2), \tag{2.13}$$

$$R_{\nu\sigma} = \frac{1}{2} \left(\partial_{\mu} \partial_{\sigma} h^{\mu}_{\nu} + \partial_{\nu} \partial^{\mu} h_{\mu\sigma} - \partial_{\nu} \partial_{\sigma} h - \Box h_{\nu\sigma} \right) + O(h^{2}), \tag{2.14}$$

$$R = \partial_{\mu}\partial_{\nu}h^{\mu\nu} - \Box h, \qquad (2.15)$$

with $h^{\mu}_{\mu} = h$, $\partial_{\mu}\partial^{\mu} = \square$. Going to Fourier space for simplicity, we find the curvature-squared terms

$$R^2 = h^{\mu\nu} h^{\alpha\beta} \mathcal{O}^{(1)}_{\mu\nu,\alpha\beta},\tag{2.16}$$

$$(R_{\mu\nu})^2 = h^{\mu\nu} h^{\alpha\beta} \mathcal{O}^{(2)}_{\mu\nu,\alpha\beta}, \qquad (2.17)$$

$$(R_{\mu\nu\rho\sigma})^2 = h^{\mu\nu}h^{\alpha\beta}\mathcal{O}^{(3)}_{\mu\nu,\alpha\beta}, \qquad (2.18)$$

where

$$\mathcal{O}_{\mu\nu,\alpha\beta}^{(1)} = (p_{\mu}p_{\nu} - p^{2}\eta_{\mu\nu})(p_{\alpha}p_{\beta} - p^{2}\eta_{\alpha\beta}), \qquad (2.19)$$

$$\mathcal{O}_{\mu\nu,\alpha\beta}^{(2)} = \frac{1}{4} \left(2p_{\mu}p_{\nu}p_{\alpha}p_{\beta} + p^{4}(\eta_{\mu\nu}\eta_{\alpha\beta} + \eta_{\mu\alpha}\eta_{\nu\beta}) - p^{2}(p_{\mu}p_{\nu}\eta_{\alpha\beta} + p_{\alpha}p_{\beta}\eta_{\mu\nu} + p_{\mu}p_{\beta}\eta_{\nu\alpha} + p_{\nu}p_{\alpha}\eta_{\mu\beta}) \right),$$
(2.20)

$$\mathcal{O}_{\mu\nu,\alpha\beta}^{(3)} = \frac{1}{4} \left(4p^4 \eta_{\mu\alpha} \eta_{\nu\beta} + 4p_{\mu} p_{\nu} p_{\alpha} p_{\beta} - 2p^2 (\eta_{\mu\alpha} p_{\nu} p_{\beta} + \eta_{\mu\beta} p_{\nu} p_{\alpha} + \eta_{\nu\alpha} p_{\mu} p_{\beta} + \eta_{\nu\beta} p_{\mu} p_{\alpha} \right). \tag{2.21}$$

Inspecting Eqs. (2.19)–(2.21), we find that the following combination vanishes at quadratic order in *any* dimension:

$$(R_{\mu\nu\rho\sigma})^2 - 4(R_{\mu\nu})^2 + R^2 = 0 + O(h^3).$$
 (2.22)

This is the familiar Gauss-Bonnet (GB) combination. The fact that it vanishes at $O(h^2)$ for arbitrary d was first noticed in [61] in the context of the low-energy limit of string theories.⁶

D. The reduced Einstein-Maxwell EFT

We conclude that, at least when the relevant physical observable is the four-photon amplitude, we can reduce the Einstein-Maxwell EFT using the $O(h^3)$ -vanishing of the Gauss-Bonnet term and Einstein's equation. The final result is

$$\begin{split} \mathcal{L}_{\text{EM},red} &= \mathcal{L}_{\text{kin}} + \hat{\alpha}_1 (F^{\mu\nu} F_{\mu\nu})^2 + \hat{\alpha}_2 F^{\mu\nu} F_{\nu\rho} F^{\rho\sigma} F_{\sigma\mu} \\ &+ \gamma \hat{C}^{\rho\sigma}_{\mu\nu} F^{\mu\nu} F_{\rho\sigma} + O(F^6,\ldots) \end{split}$$

with

$$\hat{\alpha}_{1} = \alpha_{1} + \frac{(d-4)^{2}}{4(d-2)^{2}} \alpha_{3} + \frac{8-3d}{4(d-2)^{2}} \alpha_{4}$$

$$-\frac{d^{2}+4d-16}{4(d-2)^{2}} \alpha_{5} + \frac{4-d}{4-2d} \alpha_{6},$$

$$-\frac{1}{2d-4} \alpha_{7} - \frac{3}{(d-1)(d-2)} \alpha_{8}$$

$$+\frac{(d-4)}{(d-1)(d-2)} \left(\alpha_{9} + \frac{\alpha_{10}}{2}\right), \tag{2.23}$$

$$\hat{\alpha}_2 = \alpha_2 + \alpha_4 + 4\alpha_5 - \alpha_7 + \frac{4}{d-2}\alpha_8 + \frac{2d}{d-2}\left(\alpha_9 + \frac{\alpha_{10}}{2}\right), \tag{2.24}$$

$$\gamma = \alpha_8. \tag{2.25}$$

III. BOUNDS FROM EXTREMAL BLACK HOLES AND PHOTON SCATTERING

We review the positivity bound produced by the condition that extremal black holes must decay, for any dimension $d \ge 4$. We then review the four-photon (4γ) amplitude generated by F^4 operators for any $d \ge 3$. It will be shown in Sec. VI and Appendix C that the bounds obtained from 4γ amplitudes upon discarding the t-channel graviton pole match approximately the black hole bound.

A. Positivity bound from extremal black holes

The nonrotating charged black hole (Reissner-Nordström) solution is parametrized by a mass M_{\circ} and total charge Q_{\circ} in Planck mass units. In Einstein gravity, the charge-to-mass ratio is bounded from above as

$$Z_{\circ} \equiv \frac{|Q_{\circ}|}{M_{\circ}} \le Z_{*}, \qquad Z_{*} = \sqrt{\frac{d-3}{d-2}}, \qquad (3.1)$$

beyond which the Reissner-Nordström solution would feature a naked singularity. A black hole saturating this bound, i.e., $Z_{\circ} = Z_{*}$, is said to be *extremal*.

⁶The GB combination vanishes exactly in d=3 due to the exact vanishing of the Weyl tensor. The combination is a total derivative in d=4, the Euler number density, and is thus again irrelevant for EFT.

There are compelling arguments that all black holes, including extremal ones, must be able to decay [3,27]. This conjecture is sometimes referred to as the black hole WGC, however we avoid using this term here to prevent naming confusion.

Extremal black holes can decay if the particle spectrum satisfies the WGC, i.e., if there is at least one particle satisfying (1.4) in the spectrum, in which case the black hole discharges via the Schwinger effect [62]. However, when no such particle is present in the theory, which is the case in our IR EFT where all massive particles are integrated out, the extremal black hole should still be able to decay. In such a situation, the extremal black hole can only decay into smaller black holes. This is kinematically allowed if the extremality bound deviates from the GR one. The most general condition is that the charge-to-mass ratio decreases with the mass [56].

For extremal black holes with sufficiently large radius r_h , satisfying the condition

$$r_h \gg \frac{g|q|M}{m^2},\tag{3.2}$$

the electromagnetic field is weak at the horizon, such that the Einstein-Maxwell EFT is valid. In this regime, the Einstein-Maxwell operators given in (2.6) induce a deviation to extremality; see, e.g., [27,31] and also [35,63] for higher order. It follows that the charge-to-mass ratio bound in our IR Einstein-Maxwell EFT takes the form $Z_{\circ} \leq Z$, where

$$\frac{Z}{Z_*} = 1 + C_{\rm IR} \frac{4(d-2)(d-3)^2}{(3d-7)} \left(\frac{(d-2)(d-3)}{Q_{\circ}^2} \frac{4\pi^{d-1}}{\Gamma(\frac{d-1}{2})} \right)^{\frac{1}{d-3}}.$$
(3.3)

Since the extremal black holes can decay if Z is a decreasing function of $Q_{\circ}^2 \sim M_{\circ}^2$, (3.3) implies the positivity bound

$$C_{\rm IR} > 0. \tag{3.4}$$

We can write

$$C_{\rm IR} = C_{\rm UV} + \Delta C, \tag{3.5}$$

where $C_{\rm UV}$ is the contribution from the UV operators and ΔC is the contribution produced upon integrating the massive charged particles. The expression of ΔC as a function of the EFT operator coefficients is given in Appendix C. In that calculation, we use the basis (2.6), and not the reduced basis (2.23). This is because for arbitrary d>4 the Gauss-Bonnet combination does not vanish beyond quadratic order in general, and hence, the reduction step in Sec. II C is not allowed in the black hole case.

B. Four-photon EFT

In d = 2, the photon does not propagate, and hence, our analysis does not apply. We focus on $d \ge 3$ for which the photon has d - 2 physical polarizations.

For d=3, the photon has a single polarization. There is a single independent F^4 operator which can be chosen to be $(F_{\mu\nu}F^{\mu\nu})^2$. The other possible F^4 structure satisfies $F_{\mu\nu}F^{\nu\rho}F_{\rho\sigma}F^{\sigma\mu}=\frac{1}{2}(F_{\mu\nu}F^{\mu\nu})^2$.

For d > 3, the EFT contains two independent Lorentz structures:

$$\mathcal{L}_{F^4} = \hat{\alpha}_1 (F_{\mu\nu} F^{\mu\nu})^2 + \hat{\alpha}_2 F_{\mu\nu} F^{\nu\rho} F_{\rho\sigma} F^{\sigma\mu}$$
$$= \alpha \mathcal{O} + \beta \tilde{\mathcal{O}} \tag{3.6}$$

with

$$\mathcal{O} = (F_{\mu\nu}F^{\mu\nu})^2, \tilde{\mathcal{O}} = 4F_{\mu\nu}F^{\nu\rho}F_{\rho\sigma}F^{\sigma\mu} - 2(F_{\mu\nu}F^{\mu\nu})^2, \quad (3.7)$$

where the \mathcal{O} , $\tilde{\mathcal{O}}$ basis is introduced for further convenience. The translation between the two bases is given by

$$\hat{\alpha}_1 = \alpha - 2\beta, \qquad \hat{\alpha}_2 = 4\beta. \tag{3.8}$$

Notice that for d=3, we have $\tilde{\mathcal{O}}=0$ algebraically. In d=4, we have $\tilde{\mathcal{O}}=(F_{\mu\nu}\tilde{F}^{\mu\nu})^2$ where the dual tensor is $\tilde{F}_{\mu\mu}=\frac{1}{2}\epsilon^{\mu\nu\rho\sigma}F_{\rho\sigma}$.

C. Positivity bounds from photon scattering

1. General considerations

In the absence of gravity, positivity bounds on the F^4 operators can be derived using unitarity of forward amplitudes or causality. In the presence of gravity, exploiting the forward amplitudes is complicated due to singular t-channel graviton exchange,

See [3,40,41,43,44]. A work-around to eliminate the unwanted graviton pole may be to perform an appropriate spatial compactification that removes the t-channel infrared singularity; see [44]. This approach suggests that the t-channel graviton pole may simply be discarded in the proof of the positivity bounds. It was, however, argued that the obtained results appear to be overly strong [5,6], at least in the 4d case. Another approach to the graviton pole is to work at finite impact parameter and focus on appropriate sum rules [10]. In contrast, causality bounds from low-energy photon propagation apply without extra complication in the presence of gravity. The standard F^4 positivity

bounds in d = 4 are independently obtained from causality arguments; see [64] and also [25].

Our approach in the present work is to use the most standard F^4 positivity bounds, already presented in [3],⁷ to avoid any technical digression. In doing so, we assume *a priori* that the *t*-channel pole can be neglected in the case of photon scattering, as hinted by d=4 causality bounds. This IR consistency bound will be compared to the one from extremal black hole decay, and we will find they are consistent with each other.

2. Bounds

Infrared consistency bounds on the F^4 operators are easily extended to any dimension as follows. We follow the approach of [65]. We consider the four photon amplitude $\mathcal{A}_{\gamma\gamma\to\gamma\gamma}$ with ingoing (outgoing) momentum $p_{1,2}$ ($p_{3,4}$) and ingoing (outgoing) polarization vectors $\epsilon_{1,2}$ ($\epsilon_{3,4}$). We then take the forward limit

$$\mathcal{A}_{\gamma\gamma\to\gamma\gamma}^{\mathrm{fw}} = \mathcal{A}_{\gamma\gamma\to\gamma\gamma}(p_1 = p_3, p_2 = p_4, \epsilon_1 = \epsilon_3, \epsilon_2 = \epsilon_4)$$
(3.10)

and require positivity of $\mathcal{A}_{\gamma\gamma\to\gamma\gamma}^{\text{fw}}$ for all $\epsilon_{1,2}$.

d > 3 case. The d > 3 case is analogous to d = 4. We obtain

$$\mathcal{A}_{\gamma\gamma\to\gamma\gamma}^{\mathrm{fw}} = 16\hat{\alpha}_1 s^2 (\epsilon_1 \cdot \epsilon_2)^2 + 4\hat{\alpha}_2 s^2 \left((\epsilon_1 \cdot \epsilon_2)^2 + (\epsilon_1)^2 (\epsilon_2)^2 \right) \tag{3.11}$$

$$=16\alpha s^{2}(\epsilon_{1}\cdot\epsilon_{2})^{2}+16\beta s^{2}\big((\epsilon_{1})^{2}(\epsilon_{2})^{2}-(\epsilon_{1}\cdot\epsilon_{2})^{2}\big).$$

$$(3.12)$$

From the second line, the requirement $\mathcal{A}_{\gamma\gamma\to\gamma\gamma}^{\mathrm{fw}} > 0$ for all $\epsilon_{1,2}$ implies positivity of the Wilson coefficients in the $\mathcal{O}, \tilde{\mathcal{O}}$ basis defined in $(3.6)^8$:

$$\alpha|_{d>3} \ge 0 \qquad \beta|_{d>3} \ge 0.$$
 (3.13)

d=3 case. For d=3, the photon has a single polarization, i.e., it is equivalent to a scalar. We can use (3.12) with $(\epsilon_1 \cdot \epsilon_2)^2 = 1$. $\mathcal{A}_{\gamma\gamma \to \gamma\gamma}^{\mathrm{fw}} > 0$ implies that

$$\alpha|_{d=3} \ge 0 \tag{3.14}$$

while the term multiplying β vanishes identically, in accordance with the property of the $\mathcal{O}, \tilde{\mathcal{O}}$ basis (3.6).

IV. THE ONE-LOOP EFT OF CHARGED PARTICLES

We consider the gravitational EFT of fields with spin $0, \frac{1}{2}, 1$ and with U(1) charge q. It is described by the effective Lagrangian $\mathcal{L}_{\text{eff},UV}$ that contains local higher dimensional operators involving $F_{\mu\nu}$, $R_{\mu\nu\rho\sigma}$ as well as the charged fields.

Our focus here being on the four-photon interactions induced by $\mathcal{L}_{\mathrm{eff},UV}$, it is enough to write explicitly the local F^4 operators, while neglecting the other higher-dimensional operators. The UV operator involving the charged fields would contribute only at higher order, while $R_{\mu\nu\rho\sigma}$ can be reduced along the lines of Sec. II. We have therefore the ultraviolet EFT Lagrangian

$$\mathcal{L}_{\text{eff.UV}} = \mathcal{L}_{\text{kin}} + \mathcal{L}_{F^4.\text{UV}} + \mathcal{L}_{\text{matter}}$$
 (4.1)

with

$$\mathcal{L}_{F^{4},\text{UV}} = \alpha_{\text{UV},1} (F^{\mu\nu} F_{\mu\nu})^{2} + \alpha_{\text{UV},2} F^{\mu\nu} F_{\nu\rho} F^{\rho\sigma} F_{\sigma\mu} + \gamma_{\text{UV}} \hat{C}^{\rho\sigma}_{\ \mu\nu} F^{\mu\nu} F_{\rho\sigma}. \tag{4.2}$$

The $\alpha_{\mathrm{UV},i}$, γ_{UV} coefficients are free parameters in the UV EFT. They encapsulate the effects of the dynamics of the UV completion in the sub-Planckian four-photon scattering. See Appendix A for a few known examples of contributions. In the following, we remain agnostic about $\alpha_{\mathrm{UV},i}$, γ_{UV} .

The charged particles with spin $s = 0, \frac{1}{2}, 1$ are described by the following matter Lagrangians.

Spin 0. The Lagrangian is

$$\mathcal{L}_0 = -|D_u \Phi|^2 - m^2 |\Phi|^2 - \xi |\Phi|^2 R, \tag{4.3}$$

where Φ is a complex scalar. We have $D_{\mu}\Phi=\partial_{\mu}\Phi+igqA_{\mu}\Phi$. A conformally coupled scalar has $\xi=\frac{d-2}{4(d-1)}$ in addition to m=0.

Spin $\frac{1}{2}$. The Lagrangian is

$$\mathcal{L}_{1/2} = -\frac{1}{2}\bar{\Psi}(\not D - m)\Psi, \tag{4.4}$$

where Ψ is a Dirac spinor. We have $\not D = \gamma^{\mu} D_{\mu}$ with γ^{μ} the $n \times n$ Dirac matrices in d dimensions, with $n = 2^{[d/2]}$ the dimension of spinor space [54,66].

Spin 1. In order to consistently couple a massive vector to the photon, we consider a nonlinearly realized theory with gauge group SU(2) broken to U(1). The charged gauge boson lives in the SU(2)/U(1) coset. See, e.g., [67] for

For more refined positivity bounds, see, e.g., [4–9,11–24]. ⁸The F^4 positivity bounds presented in, e.g., [25,64] take the form $4\hat{\alpha}_1 - 3\hat{\alpha}_2 > |4\hat{\alpha}_1 - \hat{\alpha}_2|$. This is equivalent to (3.13) upon translation to the $\mathcal{O}, \hat{\mathcal{O}}$ basis given in (3.8).

⁹In d=3, $F^{\mu\nu}$ transforms as a vector of SO(3). This can be seen by computing the dual tensor $F^{\mu\nu}\epsilon_{\mu\nu\rho}\equiv\partial_{\rho}\phi$, where the scalar ϕ is the only degree of freedom of $F^{\mu\nu}$.

details.¹⁰ This approach fixes unambiguously the U(1) magnetic moment of the charged vector. The Lagrangian, including a R_{ε} -type gauge fixing, is

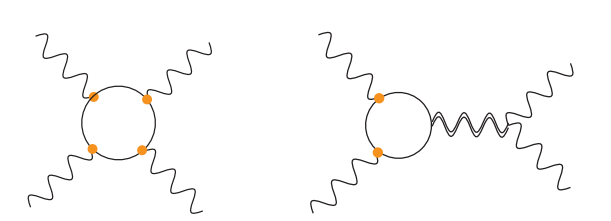
$$\mathcal{L}_{1} + \mathcal{L}_{1}^{\text{gf}} = -\frac{1}{2} |\hat{W}^{\mu\nu}|^{2} + igqF^{\mu\nu}W_{\mu}W_{\nu}^{*}$$
$$-\frac{1}{\xi_{1}} |D_{\mu}W^{\mu}|^{2} - m^{2}|W^{\mu}|^{2}, \tag{4.5}$$

where W_{μ} is the complex vector field. The field strength $\hat{W}^{\mu\nu}$ is defined as $\hat{W}^{\mu\nu} = D^{\mu}W^{\nu} - D^{\nu}W^{\mu}$, where D_{μ} is the U(1) covariant derivative. In the following, we choose the Feynman gauge $\xi_1 = 1$.

The coefficient of the U(1) magnetic moment operator $iF^{\mu\nu}W_{\mu}W_{\nu}^{*}$ can be generalized to other values since it is invariant under U(1) gauge transformations. In this work, we only use the value shown in (4.5), which is the one enforced by the underlying non-Abelian gauge symmetry.

A. Integrating out charged particles at one-loop

The leading contribution of the charged particle to the four-photon interaction is through one-loop diagrams. Three kinds of contributions appear, that are respectively proportional to $(gq)^4$, $\frac{(gq)^2}{M^{d-2}}$ and $\frac{1}{M^{2d-4}}$:





Here, the dots represent the U(1) charges, the double wiggles represent gravitons, and the internal bubbles can be of any of the charged particles.

At energy scales below the charged particle mass, the $A_{\gamma\gamma\to\gamma\gamma}$ amplitude can be described by an infrared EFT in which the massive charged particle is integrated out, as explained in Sec. II A. The generic form of the effective Lagrangian is given in Eq. (2.6).

For even spacetime dimensions, some of the diagrams in (4.6) contain UV divergences. These divergences renormalize the local F^4 operators already present in the UV effective Lagrangian. The initial value of the $\alpha_{\rm UV}$, $\beta_{\rm UV}$ coefficients is assumed to be defined from the $\mathcal{A}_{\gamma\gamma\to\gamma\gamma}$ process at Planckian energy $E\sim M$, such that the running produces logarithmic corrections of the form $\log\frac{M}{m}$ in the F^4 operators of the IR EFT.¹¹

Both the renormalization flow and the finite effects from the loops of the charged particle are encoded into the one-loop effective action. An efficient way to extract both of these bits of information is to use the well-known expansion of the effective action into heat kernel coefficients. See [47,49] for seminal papers and [48] for a review. Other useful references are [50,51,54]. Our main technical references are [48,54].

The one-loop effective action induced by the matter fields takes the form

$$\Gamma_{\text{mat}}^{(1)} = (-)^F \frac{i}{2} \text{Tr log} [(-\Box + m^2 + X)_{ij}]$$
 (4.7)

with $\Box=g_{\mu\nu}D^{\mu}D^{\nu}$ being the Laplacian built from background-covariant derivatives. The covariant derivatives give rise to a background-dependent field strength $\Omega_{\mu\nu}=[D_{\mu},D_{\nu}]$, encoding both gauge and curvature connections. It takes the general form

$$\Omega_{\mu\nu} = -iF^a_{\mu\nu}t_a - \frac{i}{2}R_{\mu\nu}{}^{\rho\sigma}J_{\rho\sigma}, \qquad (4.8)$$

where t_a and $J_{\rho\sigma}$ are the generators of the gauge and spin representation of the quantum fluctuation, respectrively. X is the "field-dependent mass matrix" of the quantum fluctuations; it is a local background-dependent quantity. The effective field strength $\Omega_{\mu\nu}$ and the effective mass X are, together with the curvature tensor, the building blocks of the heat kernel coefficients. Using the heat kernel method reviewed in Appendix D, $\Gamma_{\rm mat}^{(1)}$ takes the form

$$\Gamma_{\text{mat}}^{(1)} = (-)^F \frac{1}{2} \frac{1}{(4\pi)^{\frac{d}{2}}} \int_{\mathcal{M}} d^d x \sqrt{g} \sum_{r=0}^{\infty} \frac{\Gamma(r - \frac{d}{2})}{m^{2r - d}} \text{tr } b_{2r}(x)$$
 (4.9)

with tr the trace over internal (nonspacetime) indexes. Analytical continuation in d has been used, and the

^{1.} Expanding the one-loop effective action

¹⁰This is analogous to the W boson of the Standard Model upon decoupling the $U(1)_B$ gauge field.

¹¹The U(1) gauge coupling is not renormalized in the IR EFT, as can be verified by dimensional analysis.

expression is valid for any dimension. The local quantities b_{2r} are referred to as the heat kernel coefficients.

For odd dimensions, all the terms in Eq. (4.9) are finite. For even dimensions, there are log-divergences. These log divergences renormalize $\mathcal{L}_{\text{eff}}^{(0)}$. The terms with negative powers of masses in Eq. (4.9) are finite. They amount to an expansion for large m and give rise to the one-loop contribution to the effective Lagrangian $\mathcal{L}_{\text{eff}}^{(1)}$,

$$\mathcal{L}_{\text{eff}}^{(1)} = (-)^F \frac{1}{2} \frac{1}{(4\pi)^{\frac{d}{2}}} \sum_{r=\lfloor d/2 \rfloor + 1}^{\infty} \frac{\Gamma(r - \frac{d}{2})}{m^{2r - d}} \operatorname{tr} b_{2r}(x). \tag{4.10}$$

Only the first heat kernel coefficients are explicitly known, and the coefficients up to b_8 contribute to the observables considered in this work.

2. Spin 0

The one-loop effective action following from the Lagrangian (4.3) is

$$\Gamma_0^{(1)} = \frac{i}{2} \operatorname{Tr} \log[(-\Box + m^2 + \xi R)].$$
 (4.11)

The geometric invariants are

$$X = \xi RI, \qquad \Omega_{\mu\nu} = -igqF_{\mu\nu}. \tag{4.12}$$

3. Spin 1/2

The one-loop effective action following from the Lagrangian (4.4) is

$$\Gamma_{1/2}^{(1)} = -\frac{i}{4} \operatorname{Tr} \log \left[\left(-\Box + m^2 + \frac{1}{4} R + S^{\mu\nu} gq F_{\mu\nu} \right) \right]$$
(4.13)

with $S^{\mu\nu}=\frac{i}{4}[\gamma^{\mu},\gamma^{\nu}].$ The geometric invariants are

$$X = \frac{1}{4}R + \frac{i}{2}\gamma^{\mu}\gamma^{\nu}gqF_{\mu\nu}, \qquad \Omega_{\mu\nu} = -igqF_{\mu\nu} + \frac{1}{4}\gamma^{\rho}\gamma^{\sigma}R_{\rho\sigma\mu\nu}. \tag{4.14}$$

4. Spin 1

For the massive spin 1 particle, the contributions from the ghosts and the Goldstone boson must be included. In the Feynman gauge, these degrees of freedom are degenerate and do not mix. The ghosts contribute as -2 times a scalar adjoint with $\xi=0$. Similarly, the Goldstone contributes as +1 the scalar term [see, e.g., [54,67]]. As a result, the one-loop effective action following from the Lagrangian (4.5) is

$$\Gamma_{1}^{(1)} = \frac{i}{2} \operatorname{Tr} \log \left[\left((-\Box + m^{2}) \delta^{\mu}_{\ \nu} + R^{\mu}_{\ \nu} + 2igq F^{\mu}_{\ \nu} \right) \right] - \frac{i}{2} \operatorname{Tr} \log \left[(-\Box + m^{2}) \right], \tag{4.15}$$

where the last term is the ghost + Goldstone contribution. The geometric invariants of the vector fluctuation are

$$X^{\mu}_{\ \nu} = R^{\mu}_{\ \nu} + 2igqF^{\mu}_{\ \nu}, \qquad (\Omega_{\mu\nu})^{\rho}_{\ \sigma} = -R^{\rho}_{\ \sigma\mu\nu} - i\delta^{\rho}_{\sigma}gqF_{\mu\nu}.$$
(4.16)

B. The coefficients

The complete expressions of the heat kernel coefficients are given in Appendix D. Only a subset of terms is relevant to our study. Terms which are total derivatives can be ignored since they are irrelevant for scattering amplitudes. As explained in Sec. II, in the EFT framework, we can use the leading order equations of motion to reduce the effective Lagrangian.

The relevant pieces to compute the Einstein-Maxwell EFT are the following.

1. R² terms

The curvature squared contributions from the b_4 coefficient,

$$b_4 = \frac{1}{360} \left(5R^2 - 2R_{\mu\nu}R^{\mu\nu} + 2R_{\mu\nu\rho\sigma}R^{\mu\nu\rho\sigma} \right) I + \dots \tag{4.17}$$

with I the identity matrix for internal indexes. For our purposes, these can be further reduced using the $O(h^3)$ vanishing of the Gauss-Bonnet term; see Sec. II C.

2. RF² terms

The RF^2 contributions come from the b_6 coefficient. These are those with three powers of X, two powers of X and two derivatives, and one curvature and two powers of X. We have thus

$$b_{6} = \frac{1}{360} \left(8D_{\rho} \Omega_{\mu\nu} D^{\rho} \Omega^{\mu\nu} + 2D^{\mu} \Omega_{\mu\nu} D_{\rho} \Omega^{\rho\nu} + 12\Omega_{\mu\nu} \Box \Omega^{\mu\nu} - 12\Omega_{\mu\nu} \Omega^{\nu\rho} \Omega_{\rho}^{\ \mu} + 6R_{\mu\nu\rho\sigma} \Omega^{\mu\nu} \Omega^{\rho\sigma} - 4R_{\mu}^{\ \nu} \Omega^{\mu\rho} \Omega_{\nu\rho} + 5R\Omega_{\mu\nu} \Omega^{\mu\nu} + 60X \Box X + 30D_{\mu} X D^{\mu} X - 60X^{3} - 30X\Omega_{\mu\nu} \Omega^{\mu\nu} + 30XXR \right) + \dots$$
(4.18)

To reduce b_6 , we use the photon equation of motion (EOM), the Bianchi identities, and the Ricci identity, as detailed in Sec. II B.

3. F^4 terms

The F^4 coefficients come from the b_8 heat kernel coefficient, which can be found in Ref. [51]. Converting to Minkowski space, we have

$$b_8 = \frac{1}{24} \left(\gamma_1^{(s)} (F_{\mu\nu} F^{\mu\nu})^2 + \gamma_2^{(s)} F_{\mu\nu} F^{\nu\rho} F_{\rho\lambda} F^{\lambda\nu} \right) + \dots, \tag{4.19}$$

$$\left(\gamma_1^{(0)}, \gamma_2^{(0)}\right) = \left(\frac{1}{12}, \frac{7}{105}\right),$$
 (4.20)

$$\left(\gamma_1^{(1/2)}, \gamma_2^{(1/2)}\right) = \left(\frac{1}{3}n, -\frac{14}{15}n\right),$$
 (4.21)

$$\left(\gamma_{1}^{(V)}, \gamma_{2}^{(V)}\right) = \left(\frac{d-48}{12}, \frac{d+240}{15}\right),$$
 (4.22)

and $(\gamma_1^{(1)}, \gamma_2^{(1)}) = (\gamma_1^{(V)}, \gamma_2^{(V)}) - (\gamma_1^{(0)}, \gamma_2^{(0)})$ for the massive spin 1 particle.

C. The reduced Einstein-Maxwell effective action

Putting together the results from previous sections, we obtain the low-energy Einstein-Maxwell effective action generated by integrating out the charged particles of spin $s = 0, \frac{1}{2}, 1$. The leading contributions are encoded in the one-loop effective action, $\Gamma_s^{(1)}$.

We apply the reduction computed in (2.23). The reduced Einstein-Maxwell effective action is

$$\Gamma_{\rm IR} = \Gamma^{(0)} + \Gamma_s^{(1)} + \dots$$
 (4.23)

with

$$\Gamma^{(0)} = \int d^d x \left(\mathcal{L}_{kin} + \mathcal{L}_{F^4,UV} \right), \tag{4.24}$$

$$\Gamma_s^{(1)} = \int d^d x \Big(\Delta \hat{\alpha}_1^{(s)} (F_{\mu\nu} F^{\mu\nu})^2 + \Delta \hat{\alpha}_2^{(s)} F_{\mu\nu} F^{\nu\rho} F_{\rho\sigma} F^{\sigma\mu} + \Delta \gamma^{(s)} \hat{C}^{\rho\sigma}{}_{\mu\nu} F^{\mu\nu} F_{\rho\sigma} \Big),$$
(4.25)

$$\begin{split} \Delta \hat{\alpha}_{1,2}^{(s)} &= \frac{1}{(4\pi)^{d/2}} \left[\frac{g^4 q^4}{m^{8-d}} \Gamma \left(4 - \frac{d}{2} \right) a_{1,2}^{(s)} \right. \\ &+ \frac{g^2 q^2}{m^{6-d} M^{d-2}} \Gamma \left(3 - \frac{d}{2} \right) b_{1,2}^{(s)} \\ &+ \frac{1}{m^{4-d} M^{2d-4}} \Gamma \left(2 - \frac{d}{2} \right) c_{1,2}^{(s)} \right], \end{split} \tag{4.26}$$

$$\Delta \gamma^{(s)} = \frac{1}{(4\pi)^{d/2}} \frac{g^2 q^2}{m^{6-d} M^{d-2}} \Gamma\left(3 - \frac{d}{2}\right) d^{(s)}. \tag{4.27}$$

The coefficients for each spin are

$$a_1^{(0)} = \frac{1}{288}, \qquad a_2^{(0)} = \frac{1}{360},$$
 (4.28a)

$$a_1^{(1/2)} = -\frac{n}{144}, \qquad a_2^{(1/2)} = \frac{7n}{360},$$
 (4.28b)

$$a_1^{(1)} = \frac{d-49}{288}, \qquad a_2^{(1)} = \frac{d+239}{360}.$$
 (4.28c)

$$b_1^{(0)} = \frac{1}{720} \left[\left(30\xi - 5 + \frac{4}{(d-1)(d-2)} \right) (d-4) + \left(4 + \frac{8}{d-2} \right) \right] \frac{1}{(d-2)},$$
(4.29a)

$$b_1^{(1/2)} = -\frac{n}{720} \left[\left(-5 + \frac{4}{(d-1)(d-2)} \right) \frac{d-4}{2(d-2)} - \frac{13(d-2)-4}{(d-2)^2} \right], \tag{4.29b}$$

$$b_1^{(1)} = \frac{1}{720} \left[\left(\frac{4(d+59)}{(d-1)(d-2)} - 5(d-31) \right) \frac{d-4}{d-2} + \frac{4(d-1)(d+120)}{(d-2)^2} \right], \tag{4.29c}$$

$$b_2^{(0)} = -\frac{1}{360} \left(4 + \frac{8}{d-2} \right), \tag{4.29d}$$

$$b_2^{(1/2)} = -\frac{n}{360} \left(-\frac{4}{d-2} + 13 \right), \tag{4.29e}$$

$$b_2^{(1)} = -\frac{1}{360} \left(4(d+119) + \frac{8(d+59)}{d-2} \right). \tag{4.29f}$$

$$c_1^{(0)} = \frac{1}{720} \left[\frac{6 + \xi(\xi - \frac{1}{3})}{4} \frac{(d-4)^2}{(d-2)^2} - \frac{3(3d-8)}{(d-2)^2} \right],$$

$$c_2^{(0)} = \frac{1}{60},$$
(4.30a)

$$c_1^{(1/2)} = -\frac{n}{960} \left(\frac{3(3d-8)}{(d-2)^2} + \frac{(d-4)^2}{(d-2)^2} \right),$$

$$c_2^{(1/2)} = \frac{n}{80},$$
(4.30b)

$$c_1^{(1)} = \frac{1}{240} \left[\frac{(d-11)(d-4)^2}{2(d-2)^2} - \frac{(d+9)(3d-8)}{(d-2)^2} \right],$$

$$c_2^{(1)} = \frac{d+9}{60}.$$
(4.30c)

$$d^{(0)} = -\frac{1}{180},\tag{4.31a}$$

$$d^{(1/2)} = \frac{n}{360},\tag{4.31b}$$

$$d^{(1)} = -\frac{d+59}{180}. (4.31c)$$

Before reduction of the Einstein-Maxwell Lagrangian, our results for the RF^2 operators from spin $\frac{1}{2}$ in d=3 and from spin $0,\frac{1}{2}$ in d=4 match, respectively, those found in [53,68] and [52,68]. For d=3, the $a_{1,2}^{(0)}$ coefficients with $\xi=0$ match with [45], and for d=4, the $a_{1,2}^{(s)}$ coefficients match those from [69–71], upon appropriate conversion to the $(\mathcal{O},\tilde{\mathcal{O}})$ basis using (3.6).

1. Beta functions and logarithmic corrections

The Gamma functions in $\Delta\hat{\alpha}_{1,2}$, $\Delta\gamma$ diverge for certain even dimensions. These are physical divergences, appearing here via the framework of dimensional regularization. These divergences imply that there is a renormalization group equation associated to the corresponding local operators contained in $\Gamma^{(0)}$. In that situation, the values $\alpha_{\mathrm{UV},i}$ or γ_{UV} are understood as the values at the initial condition of the renormalization flow that we choose to be the Planck scale. That is, $\mu=M$ with μ the renormalization scale, and $\alpha_{\mathrm{UV},i}\equiv\alpha_i(M)$, $\gamma_{\mathrm{UV}}\equiv\gamma(M)$. These are the values appropriate to study the physical process $\mathcal{A}_{\gamma\gamma\to\gamma\gamma}$ with energy scale near M. To study $\mathcal{A}_{\gamma\gamma\to\gamma\gamma}$ at lower energies, the renormalization scale must be changed accordingly to minimize higher-order contributions to the one-loop prediction.

Let us compute the beta functions explicitly. Divergences occur when $r - \frac{d}{2} \sim -n$, i.e., $d \sim 2n + 2r$ with $n \in \mathbb{N}$. We define $\epsilon = 2n + 2r - d$. Introducing the renormalization scale μ in the Lagrangian, we have

$$\frac{\mu^{\epsilon}}{m^{\epsilon}} \Gamma\left(r - \frac{d}{2}\right) \xrightarrow{\epsilon \to 0} \frac{(-1)^n}{n!} 2\left(\frac{1}{\epsilon} + \log\left(\frac{\mu}{m}\right)\right). \tag{4.32}$$

Such terms from the one-loop effective action $\Gamma^{(1)}$ combine with the coefficients of the local operators in $\Gamma^{(0)}$. One absorbs the $1/\epsilon$ constant into the definitions of the coefficients, leaving only the $\log(\mu)$ dependence. The physical parameter is identified (at one-loop order) as

$$\alpha_i^{\text{phys}} = \alpha_i(\mu) + B_i \log \frac{\mu}{m}, \tag{4.33}$$

where the generic B_i coefficient is computed from (4.28)–(4.31), and analogously for γ . Requiring $\frac{d}{d\mu}\alpha_i^{\rm phys}=0$ determines the one-loop beta function for the Lagrangian parameter

$$\beta_{\alpha_i} \equiv \frac{d}{d \log \mu} \alpha_i = -B_i + O(\text{higher order loops}).$$
 (4.34)

The beta functions for the couplings of the F^4 and CF^2 operators are presented in Sec. V.

Finally, when the renormalization flow is caused by a massive particle, it stops at the scale $\mu = m$. Below this scale, we work with the IR EFT (i.e., the Einstein-Maxwell EFT) in which the only remainder of the charged particles is the set of finite contributions to the local operators [see [58]]. The coefficients in the IR EFT take the form

$$\alpha_{\text{IR},i} = \alpha_{\text{UV},i} + \Delta \alpha_i^{\text{finite}} + B_i \log \frac{M}{m}$$
 (4.35)

and analogously for γ .

V. THE F^4 BETA FUNCTIONS AND INFRARED CONSISTENCY

In this section, we assume that the charged particle is exactly massless. We compute the 1-loop beta functions and discuss the F^4 renormalization flow.

A. The beta functions

We compute the 1-loop beta functions of the F^4 and CF^2 operators along the lines presented in Sec. IV C 1. For a massless spin-1 particle, the corresponding heat kernel coefficients are given by $a_i^{(1)} = a_i^{(V)} - 2a_i^{(0)}$. At zero mass, the only beta functions of the F^4 operators appear for d = 4, 6, and 8. They are given in Tables I–III.

In d = 4, graviton and photon loops produce an additional contribution to the R^2 operators. Note these are the loops that cause the d = 4 conformal anomaly in the IR

TABLE I. Beta function of the α coefficient.

		Spin	
d	0	$\frac{1}{2}$	1
4	$-\frac{19}{480\pi^2}\frac{1}{M^4}$	$-\frac{13}{320\pi^2}\frac{1}{M^4}$	$-\frac{29}{640\pi^2}\frac{1}{M^4}$
6	$\frac{23-50\xi}{76800\pi^3} \frac{g^2q^2}{M^4}$	$\frac{13}{4800\pi^3} \frac{g^2 q^2}{M^4}$	$\frac{661}{38400\pi^3} \frac{g^2 q^2}{M^4}$
8	$-\frac{7}{184320\pi^4}g^4q^4$	$-\frac{1}{2880\pi^4}g^4q^4$	$-\frac{47}{30720\pi^4}g^4q^4$

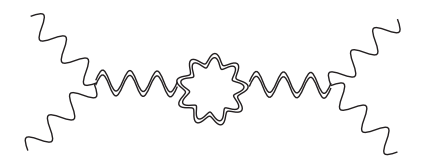
TABLE II. Beta function of the β coefficient.

		Spin	
d	0	$\frac{1}{2}$	1
4	$-\frac{19}{480\pi^2}\frac{1}{M^4}$	$-\frac{13}{320\pi^2}\frac{1}{M^4}$	$-\frac{29}{640\pi^2}\frac{1}{M^4}$
6	$\frac{1}{7680\pi^3} \frac{g^2 q^2}{M^4}$	$\frac{1}{480\pi^3} \frac{g^2 q^2}{M^4}$	$\frac{13}{960\pi^3} \frac{g^2 q^2}{M^4}$
8	$-\frac{1}{184320\pi^4}g^4q^4$	$-\frac{7}{11520\pi^4}g^4q^4$	$-\frac{41}{30720\pi^4}g^4q^4$

TABLE III. Beta function of the γ coefficient in d = 6.

Spin	0	$\frac{1}{2}$	1
	$\frac{1}{5760\pi^3} \frac{g^2 q^2}{M^4}$	$-\frac{1}{1440\pi^3}\frac{g^2q^2}{M^4}$	$\frac{13}{1152\pi^3} \frac{g^2 q^2}{M^4}$

EFT [see, e.g., [48,72]]. Following Sec. II B, in the Einstein-Maxwell EFT, these loops of gravitons and photons contribute to the renormalization flow of the F^4 operators via diagrams such as



The corresponding graviton contribution to the b_4 coefficient is

$$b_4^{\text{grav}} = \frac{1}{180} \left(414 R_{\mu\nu}^2 + \frac{553}{4} R^2 \right)$$
$$= \frac{23}{10} \left(F^{\mu\nu} F_{\nu\rho} F^{\rho\sigma} F_{\sigma\mu} - \frac{1}{4} (F^{\mu\nu} F_{\mu\nu})^2 \right), \tag{5.1}$$

where we have used the Gauss-Bonnet identity (2.22) and the leading-order Einstein equation (2.9). This corresponds to $4\beta_{\tilde{\alpha}_1}^{\rm grav} = -\beta_{\tilde{\alpha}_2}^{\rm grav} = \frac{23}{160\pi^2}$. Translating to the $\mathcal{O}, \tilde{\mathcal{O}}$ basis, we obtain the contributions

$$\boldsymbol{\beta}_{\alpha}^{\text{grav}} = \boldsymbol{\beta}_{\beta}^{\text{grav}} = -\frac{23}{640\pi^2}.$$
 (5.2)

The photon loop contributes by an additional $\frac{1}{2}a_i^{(1)}$, where the $\frac{1}{2}$ accounts for the photon being a real vector. Due to the fact that the graviton and photon are massless, such loops do not contribute to the running of F^4 in other dimensions.

B. Discussion

Whenever the charged particle is massless or if $m \ll M$, the coefficients of the F^4 operators at low-energy scales are controlled by their beta functions. The renormalization flow washes away any finite correction, that becomes negligible compared to large logarithms. When m=0, the running coefficients at $\mu \ll M$ is

$$\alpha_i(\mu) \approx B_i \log \frac{M}{\mu}$$
 (5.3)

From Tables I and II, we can see that $\beta|_{d=4}$ and $\beta|_{d=8}$ are negative for loops of all spins. Therefore, in d=4, 8, the coefficients of the \mathcal{O} , $\tilde{\mathcal{O}}$ operators tend to grow positively when the theory flows towards the infrared. It would be tempting to conclude that the renormalization flow tends to

make the theory infrared-consistent. However, the positivity bounds we are using strictly require $m \neq 0$ and thus do not apply in the present case.

In fact, the opposite behavior appears in d=6. The spin $\frac{1}{2}$ and 1 beta functions are *positive* for both α and β coefficients. The scalar beta function for the β coefficient is positive, as is the beta function for α if $\xi < \frac{23}{50}$. This includes the conformal coupling value in d=6, $\xi=\frac{1}{5}$. These positive beta functions imply that the coefficients of the \mathcal{O} , $\tilde{\mathcal{O}}$ operators are driven towards *negative* values at sufficiently low energy scales. If positivity bounds applied at m=0, they would be necessarily violated in the deep IR, implying that the gravitational EFTs of massless particles in d=6 are infrared-inconsistent. Such a strong conclusion is avoided if none of the positivity bounds apply for m=0.

Nevertheless, we will see in next section that, in the presence of a small nonzero mass, the positivity of $\beta|_{d=6}$ tends to create a tension with the positivity bounds. It would be interesting to find if other ingredients like a gravitino or nonminimal couplings can make the beta function negative, along the lines of [33]. 12

Finally, we find that the sign of the beta function of the CF^2 operator, given in Table III, depends on the spin. This has no consequence for the positivity bounds we are using. The sign of the γ coefficient is irrelevant in the positivity bounds given in, e.g., [44], which involve $|\gamma|$, and in the present work we use a simpler positivity bound that is independent on γ .

The beta function for the C coefficient of the extremality relation, defined in (3.3), follows the same sign pattern as β_{α} and β_{β} .

VI. FINITE CORRECTIONS AND INFRARED CONSISTENCY

In this section, we assume that the charged particle is massive, m > 0. Photon scattering at energy scales below m is described by the infrared EFT, that encodes the finite corrections induced when integrating out the charged particle.

For any even dimension, at least some of the coefficients of the IR EFT receive logarithmic corrections that are large when $m \ll M$. Some of these logarithmic corrections correspond to the beta functions presented in Sec. V. The renormalization flow of the massless case is recovered when taking $m \to 0$ at finite energy or finite μ , and the only difference occurs in the spin-1 case since there is no Goldstone boson in the massless case. ¹³

The contributions to the F^4 Wilson coefficients in the IR EFT take the form

¹³The other corrections simply do not exist in the $m \to 0$ limit, since the charged particle is not integrated out.

¹²We mention that the *a*-theorem in d = 6 also presents an unexpected behavior compared to d = 2, 4; see [73,74].

$$\Delta \alpha = a \frac{g^4 q^4}{m^{8-d}} + b \frac{g^2 q^2}{m^{6-d} M^{d-2}} + \frac{c}{m^{4-d} M^{2d-4}}.$$
 (6.1)

We define a reduced notation that is used throughout this section.

A. Reduced notation

The corrections induced by the charged particles are second order polynomials in q^2 ; see (6.1). In terms of the charge-to-mass ratio z introduced in (1.4), we have

$$\Delta \alpha = \frac{1}{m^{4-d} M^{2d-4}} \left(az^4 + bz^2 + c \right), \qquad z = \frac{g|q|}{m} M^{\frac{d-2}{2}}.$$
(6.2)

Note that $[g] = 2 - \frac{d}{2}$ and hence z is dimensionless for any d.

We further define the loop factor

$$K_d = \begin{cases} 2^d \pi^{\frac{d}{2}} & \text{if } d \text{ even} \\ 2^d \pi^{\frac{d-1}{2}} & \text{if } d \text{ odd} \end{cases}$$
 (6.3)

and work with a scaled dimensionless version of (6.2), given by

$$\Delta \bar{\alpha} = \bar{a}z^4 + \bar{b}z^2 + \bar{c} \equiv K_d m^{4-d} M^{2d-4} \Delta \alpha. \quad (6.4)$$

Similar definitions hold for $\bar{\alpha}_{IR}$, $\bar{\alpha}_{UV}$, $\beta_{\bar{\alpha}}$ and for the β coefficients (i.e., $\Delta \bar{\beta}$, $\bar{\beta}_{IR}$, $\bar{\beta}_{UV}$, and $\beta_{\bar{\beta}}$). The infrared consistency condition (3.13) is equivalent to

$$\bar{\alpha}_{IR} \ge 0, \qquad \bar{\beta}_{IR} \ge 0.$$
 (6.5)

B. General analysis of positivity

The $\bar{\alpha}_{\rm IR}(z)$ polynomial is defined on \mathbb{R}_+ . Due to this restricted domain, studying the positivity of $\bar{\alpha}_{\rm IR}(z)$ requires distinguishing various cases that we classify here.

Let $\bar{\alpha}^*$ be the rightmost extremum of the quartic polynomial $\Delta \bar{\alpha}(z)$, namely,

$$\bar{\alpha}^* = \begin{cases} \bar{c}, & \text{if } \bar{a} \, \bar{b} \ge 0\\ \frac{4\bar{a} \, \bar{c} - \bar{b}^2}{4\bar{a}}, & \text{if } \bar{a} \, \bar{b} < 0, \end{cases}$$
(6.6)

and let $0 \le z_1 \le z_2$ be the two roots of $\bar{\alpha}_{IR}(z)$ in \mathbb{R}_+ .

Depending on the coefficients, the positivity constraint (6.5) imposes restrictions on the charge-to-mass ratio z, which are classified into the following cases.

- (1) Case $\bar{a} > 0$
 - (a) If $\bar{\alpha}_{UV} \ge -\bar{\alpha}^*$, then we have that $\bar{\alpha}_{IR} \ge 0$ holds for all $z \ge 0$.
 - (i) Case $\bar{b} \ge 0$

If $\bar{\alpha}_{\rm UV} < -\bar{\alpha}^* = -\bar{c}$, then there is a lower bound on z in the form $z \ge z_2 > 0$.

(ii) Case $\bar{b} < 0$

If $\bar{a}_{UV} < -\bar{c}$, then there is a lower bound on z in the form $z \ge z_2 > 0$.

If $-\bar{c} \le \bar{\alpha}_{\text{UV}} < -\bar{\alpha}^*$, then there is another allowed region for z, so that $z \in [0, z_1] \cup [z_2, \infty)$.

- (2) Case $\bar{a} < 0$
 - (a) If $\bar{\alpha}_{\rm UV} < -\bar{\alpha}^*$, then the infrared consistency condition is violated (i.e., $\bar{\alpha}_{\rm IR} < 0$ for all $z \ge 0$). In this case, we say that this value for $\bar{\alpha}_{\rm UV}$ is *excluded*.
 - (i) Case $\bar{b} \ge 0$

If $\bar{\alpha}_{\text{UV}} \ge -\bar{c}$, then there is an upper bound on z in the form $0 \le z \le z_2$.

If $-\bar{\alpha}^* \le \bar{\alpha}_{\text{UV}} < -\bar{c}$, then there is a lower and an upper bound on z in the form $z_1 \le z \le z_2$.

(ii) Case $\bar{b} < 0$

If $\bar{\alpha}_{\text{UV}} \ge -\bar{\alpha}_* = -\bar{c}$, then there is an upper bound on z in the form $0 \le z \le z_2$.

Case (1) with sufficiently small $\bar{\alpha}_{UV}$ implies the existence of a WGC-like bound on z. Conversely, in case (2) with sufficiently large $\bar{\alpha}_{UV}$, z gets always bounded in a finite region.

For d>3, we need to consider these conditions for both \mathcal{O} , $\tilde{\mathcal{O}}$ operators, i.e., for both $\bar{\alpha}_{\mathrm{IR}}$, $\bar{\beta}_{\mathrm{IR}}$ coefficients, so that the most restrictive condition dominates. The above analysis applies whether or not logarithmic contributions are present. This is because the logarithms depend only on the scale ratio $\frac{m}{M}$, which can be treated as an independent quantity with respect to the charge-to-mass ratio z. Also, for $d \geq 8$, the logarithms factor out of the entire polynomial and are thus irrelevant for the positivity analysis.

C. Positivity bounds and the WGC

This section presents the synthesis of our results for the relations between positivity bounds and the WGC. We consider the positivity bounds from infrared consistency of $\gamma\gamma \to \gamma\gamma$ ($\alpha_{\rm IR} \ge 0$, $\beta_{\rm IR} \ge 0$), discussed in Sec. III C, and those from extremal black hole decay ($C_{\rm IR} > 0$), discussed in Sec. III A. We remind readers that, here, WGC means specifically that there exists a nonzero O(1) lower bound for the charge-to-mass ratio, i.e., $z \ge z_* > 0$ [see (1.4)].

Part of our focus is the dependence of the various relations with respect to spacetime dimension. As argued in Sec. I, we take the viewpoint that dimensional dependence is a test of robustness. A relation that holds in any d might be profound, while one that only holds for certain d may be viewed as more coincidental. The systematic analyses for each dimension are collected in Appendixes B and C.

The positivity bounds from IR consistency and black hole decay are fundamentally different. The latter does not apply for d=3 and is still a conjecture, while the former is rigorous.¹⁴ Yet, both $C_{\rm IR}$ and $\alpha_{\rm IR}$, $\beta_{\rm IR}$ are quadratic in z^2 ,

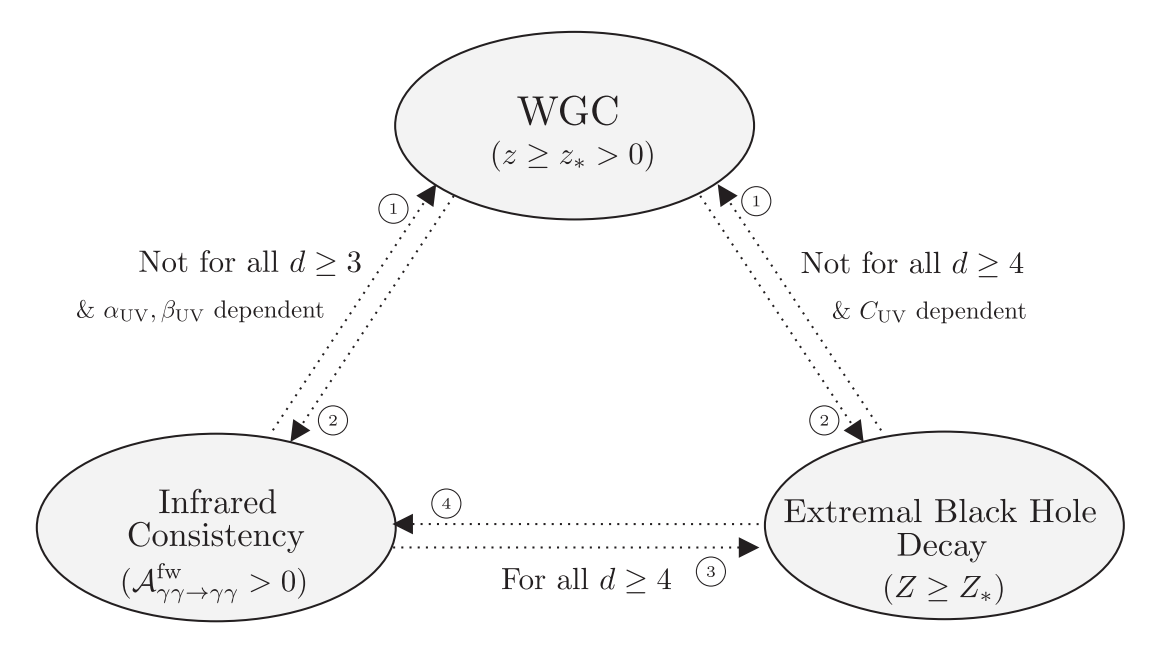
¹⁴Another difference is that the IR consistency bounds are nonstrict while the black hole bound is strict. This has no practical consequences.

and hence, we can apply the analysis of Sec. VI B to all of them. Their relations to the WGC-like bounds turn out to be very similar, hence we summarize them together.

1. Results for $d \leq 11$

The results for $\Delta \alpha$, $\Delta \beta$ and ΔC , and the condition on $\bar{\alpha}_{\rm UV}$, $\bar{\beta}_{\rm UV}$ for the WGC-like bounds on z to exist, are collected and discussed systematically in Appendixes B and C for spacetime dimensions from d=3 to d=11. In the scalar case, the positivity bounds are presented as exclusion regions in the $z\xi$ -plane; see Figs. 1–4.

We summarize the results using the following diagram:



Each of the implication arrows in this diagram come with conditions that are detailed below. The annotations summarize the essential message.

- ① Infrared consistency and extremal black hole decay both imply a WGC-like bound for d=3,4,5,7,8,11, for any spin, if $\bar{\alpha}_{\rm UV}$, $\bar{\beta}_{\rm UV}$, $\bar{C}_{\rm UV}$ are sufficiently small or negative. In these dimensions, $\Delta\alpha$, $\Delta\beta$, ΔC are positive for large enough z; i.e., case (1a) or (1b) of the general analysis (see VIB) applies. In sharp contrast, for d=9, 10, IR consistency does *not* imply a WGC-like bound. In these dimensions, $\Delta\alpha$, $\Delta\beta$, ΔC are negative at large enough z; i.e., case (2a) or (2b) applies, such that z is bounded in a finite region.
- ② The WGC implies IR consistency and extremal black hole decay for $d=3,\ 4,\ 5,\ 7,\ 8,\ 11$, unless $\bar{\alpha}_{\rm UV},$ $\bar{\beta}_{\rm UV},\ \bar{C}_{\rm UV}$ are too negative. For $d=9,\ 10$, the positivity bounds are respected only if the UV coefficients are positive and large enough for a given z. A remarkable consequence is that, in $d=9,\ 10$, the WGC does *not* imply that extremal black holes can decay in the IR EFT—this instead must be ensured by the presence of sufficiently positive Planckian F^4 operators.

- ③ Infrared consistency implies approximately the extremal black hole decay condition for any $d \ge 4$, independently of the UV operators.
- ⓐ Extremal black hole decay implies approximately the α_{IR} > 0 condition from IR consistency for any d ≥ 4, independently of the UV operators.

The implications ③, ④ are approximate in the sense that the expressions for $\Delta\alpha$ and ΔC have O(1) differences in the z^2 and z^0 coefficients, however, without qualitative implications. This can be seen directly at the level of the expressions for $\Delta\alpha$, ΔC in Appendixes B and C. As an example, for spin $\frac{1}{2}$ in d=5, the bound on z for negligible UV operators is $z\geq 2.77$ from the IR consistency condition (see Table IX), while it is $z\geq 2.78$ from the black hole condition (see Table XXIV).

In the special case of d=6, we find that implication ① produces WGC-like bounds that are enhanced by a $\sqrt{\log \frac{M}{m}}$ factor. This happens for spin $\frac{1}{2}$, 1, and 0 with $\xi > \frac{50}{23}$

¹⁵The implications ③ and ④ can also be studied at the level of the EFT coefficients. In particular, it would be interesting to investigate the connection to the compactified bounds of [44], that are slightly stronger than Eq. (3.13). The generalization to d > 4 requires a thorough analysis that we leave for future work.

in the $\Delta \bar{\alpha}$ case and is a manifestation of the positive beta functions found in Sec. V (see Appendix B and Table XII). Conversely, from implication ②, we conclude that there exists a WGC-like bound that ensures that the d=6 IR EFT is infrared-consistent and that extremal black holes can decay.

2. Results for d > 11

For d > 11, a pattern appears. The higher dimensional cases are qualitatively analogous to the cases d = 8, 9, 10, 11, mod 4. Furthermore, the cases d = 8 and 11 (respectively, d = 9 and 10) are also similar to each other, up to the overall factor $\log \frac{M}{m}$ which does not imply significant changes. Each of the analogous cases has the same sign pattern for \bar{a} , \bar{b} , and \bar{c} .

- (i) d=8+4n (respectively, d=11+4n), n=1,2,3..., is analogous to d=8 (respectively, d=11). Assuming $\bar{\alpha}_{\rm UV},\bar{\beta}_{\rm UV},\bar{C}_{\rm UV}$ are zero, z is unbounded for any spin. ¹⁶
- (ii) d = 9 + 4n (respectively, d = 10 + 4n), n = 1, 2, 3, ..., is analogous to d = 9 (respectively, d = 10). Similar to d = 9 and 10, taking vanishing $\bar{\alpha}_{\text{UV}}, \bar{\beta}_{\text{UV}}, \bar{C}_{\text{UV}}$ implies a violation of the positivity constraint for any spin. Nonzero positive $\bar{\alpha}_{\text{UV}}, \bar{\beta}_{\text{UV}}$ (respectively \bar{C}_{UV}) are then mandatory to ensure IR consistency (respectively extremal black hole decay).

VII. SUMMARY

We computed the four-photon operators generated by charged particles in any dimension in the presence of gravity. We then used consistency conditions from four-photon scattering and extremal black holes to derive a set of bounds on the gravitational EFTs of charged particles.

The general setup is a sub-Planckian (i.e., UV) gravitational EFT of a U(1) charged particle of spin $0, \frac{1}{2}$, or 1. The EFT Lagrangian features local F^4 operators that encode the effects of the UV completion of quantum gravity on fourphoton scattering. We briefly review some realizations of these UV F^4 operators from strings and branes.

We computed the effect of loops of charged particles within the UV EFT, with focus on their contributions to four-photon scattering. From a diagrammatic viewpoint, besides nongravitational box diagrams that generate F^4 operators, triangles and bubbles of charged particles attached to gravitons generate RF^2 and R^2 operators. We compute the effect of all these loops directly via expansion of the one-loop effective action encoded in the heat kernel coefficients.

The one-loop divergences of the effective action renormalize the F^4 , RF^2 and R^2 operators in certain dimensions.

Furthermore, in the case of massive charged particles, the one-loop effective action provides the IR EFT in which charged particles are integrated out. Following the standard rules of EFT, the basis of the F^4 , RF^2 , and R^2 operators can be reduced, to some extent, using the equations of motion, i.e., field redefinitions.

Our focus is ultimately on the physical process of fourphoton scattering. Gravitons contribute at one-loop, but without self interactions—to the exception of diagrams that renormalize R^2 operators in d=4. We further use that the Gauss-Bonnet combination of R^2 operators vanishes at quadratic order of graviton fluctuation in *any* dimension. The combination of these two facts implies that the basis of EFT effective operators can be reduced to F^4 and CF^2 operators in any dimension in the calculation of 4γ amplitudes.

We provide the general result for the reduced one-loop effective action for charged particles of spin $0, \frac{1}{2}$, or 1 in any dimension. Gravity induces a renormalization flow of the F^4 operator in d=4, 6, 8 and of CF^2 in d=6 dimensions. We verified the consistency of our results with some independent results on d=3, 4 Einstein-Maxwell theory from [52,53,68,70,71].

Turning to positivity bounds, we compute four-photon scattering in any $d \ge 3$, and apply a standard infrared consistency argument that provides positivity bounds on the F^4 operators. We also compute the bound produced by the condition that extremal black holes can decay in any dimension $d \ge 4$ [27]. We find that both approaches yield nearly equivalent results, even though in the amplitudes we discard the graviton t-channel pole and use the vanishing of the Gauss-Bonnet term at quadratic order for any d. The bound obtained without the graviton t-channel is also supported by independent results from causality in d = 4 [64].

The infrared consistency of four-photon scattering and the decay of extremal black holes put bounds on the UV EFT of charged particles, our results are as follows.

In d=4 and d=8, the F^4 beta functions are negative, driving F^4 to positive values in the infrared. In contrast, the d=6 beta function from spin $0, \frac{1}{2}$, and 1 drives the F^4 toward negativity. While for a massless particle, the F^4 operator flows to arbitrarily large and negative in the infrared; there is no immediate inconsistency because our positivity bounds do not apply for strictly zero m. Still, it would be interesting to find if some additional ingredient can reverse the beta function sign, for example, due to the gravitino or nonminimal couplings along the lines of [33].

For massive charged particles, we investigate the positivity bounds on the IR EFT in any dimension, with specific focus on d from 3 to 11. Our results always depend on the value of the UV F^4 operators encapsulating unknown super-Planckian effects. We remain agnostic to its value $a\ priori$, but for concreteness we discuss cases where it is either negligible or large and positive.

¹⁶For spin 0, the bounds on z become independent of ξ ; i.e., when $n \ge 1$, the exclusion region analogous to Fig. 4 becomes empty.

The F^4 positivity bounds can constrain the charge-tomass ratio z provided the UV F^4 coefficients are not too large and positive. The quantities constrained are quadratic polynomials in z^2 defined on \mathbb{R}_+ . A variety of bounds appear depending on the shape of these polynomials. The bounds on z can be from above or below and can be one or two-sided, and disjoint domains are also possible.

For d=3, 4, 5, 7, 8, 11, we find that the positivity bounds imply O(1) lower bounds on z similar to the d-dimensional weak gravity conjecture for any spin, and for sufficiently small or negative $\bar{\alpha}_{\rm UV}$, $\bar{\beta}_{\rm UV}$. We systematically present the condition on $\bar{\alpha}_{\rm UV}$, $\bar{\beta}_{\rm UV}$ for the WGC-like bounds on z to exist. The bounds on the scalar depend on ξ except in d=4; they are presented as exclusion regions in the $z\xi$ -plane.

In the specific case of vanishing $\bar{\alpha}_{\rm UV}$, $\bar{\beta}_{\rm UV}$, or $C_{\rm UV}$, neat WGC-like bounds appear, for example, in d=5 for all spins. This feature is not general, however. For instance, in d=3, the spin 0 and spin $\frac{1}{2}$ cases remain unbounded. This conclusion differs from the one from [40], but simply because the finite contribution from R^2 was ignored or equivalently absorbed into the UV coefficient in this reference.

For d=6, the positivity bounds produce WGC-like bounds that are enhanced by a $\sqrt{\log \frac{M}{m}}$ factor. This happens for spin $\frac{1}{2}$, 1, and 0 with $\xi > \frac{50}{23}$ in the $\Delta \bar{\alpha}$ case, and it is a manifestation of the positive beta functions found in d=6.

Finally, for d=9, 10, it turns out that the logic is different. The UV coefficient must be large enough for positivity bounds to be satisfied for a given value of z. In these cases, z is bounded in a finite range. As a result, even if the UV coefficients are very large, there is necessarily an upper bound on the charge multiplied by a power of mass. For higher dimensions, similar cases arise following a mod 4 pattern. A remarkable implication of these d=9, 10 results is that the WGC does *not* imply extremal black hole decay in the IR EFT.

A general takeaway from our study is that the connection between positivity bounds (from IR consistency, extremal black hole decay) and the WGC may not be so profound, as it appears to be strongly dimension-dependent.

On the other hand, the approximate correspondence that we observe in any dimension between the IR consistency bounds and extremal black hole decay deserves further investigation. In d=4, it can be noticed that an IR consistency bound obtained via the compactification method of [44], which is slightly more stringent than the one used here, turns out to match precisely the extremal black hole bound once both electric and magnetic cases are taken into account. It would be very interesting to verify whether this correspondence persists in d>4, that would likely hold only up to $O(\frac{1}{M^4})$ corrections due to the nonvanishing Gauss-Bonnet contribution to the extremality relation. This investigation requires, however, a thorough

analysis of the compactification method for higher d, that we leave for future work.

ACKNOWLEDGMENTS

We thank Dmitri Vassilievich for useful discussions and Benjamin Knorr, Javi Serra, Junsei Tokuda, Congkao Wen, and collaborators for valuable correspondence. This work was supported in part by the São Paulo Research Foundation (FAPESP), Grant No. 2021/10128-0. The work of P. B. was supported by Coordination for the Improvement of Higher Education Personnel—Brazil (CAPES)—Finance Code 88887.816450/2023-00, and L. d. S. was supported by Grant No. 2023/11293-0 of FAPESP.

DATA AVAILABILITY

No data were created or analyzed in this study.

APPENDIX A: EXAMPLES OF F^4 OPERATORS FROM STRINGS AND BRANES

The ultraviolet F^4 operators are generated in string theory. For example, the four-photon interaction arising at low-energy from perturbative open string amplitude in d=10, at lowest order in the string coupling g_s , can be found in [75,76]. For large string tension $\frac{1}{2\pi\alpha'_s}$, we deduce from the string amplitude the following effective Lagrangian [see also [77]]:

$$\mathcal{L}_{F^4,\text{string}} = \frac{1}{8} g_s (2\pi\alpha_s')^2 \left(F^{\mu\nu} F_{\nu\rho} F^{\rho\sigma} F_{\sigma\mu} - \frac{1}{4} (F^{\mu\nu} F_{\mu\nu})^2 \right) + O(\alpha_s'^4). \tag{A1}$$

The prediction holds under the compactification of spatial dimensions; however, in that case, contributions from the Kaluza-Klein modes should also be taken into account, which likely dominate the low-energy F^4 operators.

The ultraviolet F^4 operators also appear in models where the photon arises from a D-brane, and charged particles correspond to open strings attached to the brane. This configuration was shown in [78] to be described by a Born-Infeld action. We deduce the effective Lagrangian [see also [79]]¹⁷:

$$\mathcal{L}_{BI} = -b^2 \sqrt{-\det\left(\eta_{\mu\nu} + \frac{1}{b}F_{\mu\nu}\right)} + b^2 \sqrt{-\det(\eta_{\mu\nu})}$$
(A2)
$$= -\frac{1}{4}F^{\mu\nu}F_{\mu\nu} + \frac{1}{8b^2} \left(F^{\mu\nu}F_{\nu\rho}F^{\rho\sigma}F_{\sigma\mu} - \frac{1}{4}(F^{\mu\nu}F_{\mu\nu})^2\right) + O(b^{-3}).$$
(A3)

$$\overline{1^7}$$
In $d=4$, we recover the original BI Lagrangian $\mathcal{L}_{\rm BI}=b^2\Big(1-\sqrt{1+\frac{1}{2b}F^{\mu\nu}F_{\mu\nu}-\frac{1}{4b^2}(\tilde{F}^{\mu\nu}F_{\mu\nu})^2}\Big)$ [80].

In the result of [78], upon suitable field normalization, one obtains $b^{-2} = g_s(2\pi\alpha_s')$ that exactly reproduces the overall coefficient in $\mathcal{L}_{F^4,\text{string}}$.

Once expressed in the \mathcal{O} , $\tilde{\mathcal{O}}$ basis, the specific combination of F^4 operators generated by the string models implies

$$\alpha_{\rm UV} = \beta_{\rm UV} > 0 \tag{A4}$$

in any dimension. Such a positivity bound is not surprising. Since string theory must be a consistent completion of quantum gravity, the Planckian F^4 operators have to satisfy the positivity bound regardless of the presence of light fields in the theory, which implies Eq. (A4).

The F^4 operator can also appear in compact extra dimension models with the photon localized on a brane. In that case, a universal tree-level contribution comes from the Kaluza-Klein graviton exchange, i.e., the massive version of the tree diagram (3.9). Each massive graviton $h_{\mu\nu}^{(n)}$ couples to the brane-localized photon stress tensor, $\int_{\text{brane}} \sqrt{g}_{\text{ind}} h_{\mu\nu}^{(n)} T^{\mu\nu}$. The F^4 operators are generated by integrating out the massive gravitons, whose propagator is $G_{\mu\nu,\rho\sigma}^{(n)} = \frac{-i}{p^2 + m_n^2} (\frac{1}{2} (P_{\mu\rho}^{(n)} P_{\nu\sigma}^{(n)} + P_{\mu\sigma}^{(n)} P_{\nu\rho}^{(n)}) - \frac{1}{d-1} P_{\mu\nu}^{(n)} P_{\rho\sigma}^{(n)})$ with $P_{\mu\nu}^{(n)} = \eta_{\mu\nu} - \frac{p_{\mu}p_{\nu}}{m_n^2}$. In the EFT, these massive gravitons generate the operator

$$\mathcal{L}_{\text{grav}} \propto T^{\mu\nu} T_{\mu\nu} - \frac{1}{d-1} T^2$$

$$\propto F^{\mu\nu} F_{\nu\rho} F^{\rho\sigma} F_{\sigma\mu} - \frac{d+8}{16(d-1)} \left(F^{\mu\nu} F_{\mu\nu} \right)^2. \tag{A5}$$

The subsequent $\alpha_{\rm UV}$, $\beta_{\rm UV}$ coefficients turn out to be positive for any $d \geq 3$. In the d=4 case, the combination becomes $F^{\mu\nu}F_{\nu\rho}F^{\rho\sigma}F_{\sigma\mu} - \frac{1}{4}F^{\mu\nu}F_{\mu\nu}$ as in the string case. This matches the results from [67,81].

Even though the above results suggest positivity of the $\alpha_{\rm UV},~\beta_{\rm UV}$ coefficients in the ultraviolet EFT, we should keep in mind that negative contributions do exist, for instance, from charged KK modes, as can be seen from our massive results from Sec. VI. In this work, we do not systematically evaluate the contributions that appear upon compactification. Our approach is to remain fully agnostic about the values of $\alpha_{\rm UV},~\beta_{\rm UV}.$

APPENDIX B: DETAILED BOUNDS FROM INFRARED CONSISTENCY

We discuss the consequences of IR consistency for each spacetime dimension. The results follow a pattern at large dimension. Lower dimensions require separate discussion, and we cover the cases from d=3 to d=11. In the following, we report systematically the implications of the positivity bounds (6.5) while remaining agnostic about the values of $\alpha_{\rm UV}$, $\beta_{\rm UV}$.

TABLE IV. Reduced coefficient $\Delta \bar{\alpha}$ in d = 3.

Spin	\Deltaar{lpha}
0	$\frac{7z^4}{1920} + \frac{(1-10\xi)z^2}{480} + \frac{60\xi^2-20\xi+3}{480}$
$\frac{1}{2}$	$\frac{z^4}{240} - \frac{z^2}{480} + \frac{1}{240}$
1	$\frac{127z^4}{960} - \frac{11z^2}{60} + \frac{1}{30}$

TABLE V. Condition for the existence of IR consistency bounds on the charge-to-mass ratio z and IR consistency bounds on z if $\bar{\alpha}_{\rm UV}=0$ in d=3.

Spin	Condition for z bounded	Bound if $\bar{\alpha}_{UV} = 0$
0	$\bar{\alpha}_{\rm UV} < \begin{cases} -\frac{60\xi^2 - 20\xi + 3}{480} & \text{if } \xi \le \frac{1}{10} \\ -\frac{16\xi^2 - 6\xi + 1}{168} & \text{if } \xi > \frac{1}{10} \end{cases}$	Unbounded
$\frac{1}{2}$	$\bar{\alpha}_{\mathrm{UV}} < -\frac{1}{256}$	Unbounded
1	$\bar{\alpha}_{\mathrm{UV}} < \frac{23}{762}$	$z \le 0.464 \text{ or } z \ge 1.08$

1. Case d = 3

The values of $\Delta \bar{\alpha}$ are presented in Table IV. We remind readers that there is only one independent operator in d=3, chosen to be $F_{\mu\nu}F^{\mu\nu}$ with reduced coefficient $\bar{\alpha}_{\rm IR}=\bar{\alpha}_{\rm UV}+\Delta\bar{\alpha}$.

From Table IV, we have $\bar{a}>0$, $\bar{c}>0$ for all spins, $\bar{b}<0$ for spin $\frac{1}{2}$ and 1, and $\mathrm{sign}(\bar{b})=\mathrm{sign}(1-10\xi)$ for spin 0. Therefore, cases (1a) and (1b) from the classification in Sec. VI B apply. It follows that the positivity bound $\bar{\alpha}_{\mathrm{IR}}\geq 0$ can constrain the charge-to-mass ratio z depending on the value of the UV coefficient $\bar{\alpha}_{\mathrm{UV}}$. The exact condition for the existence of a bound on z is shown in Table V.

We see that for spin $\frac{1}{2}$, and for spin 0 with any ξ , $\bar{\alpha}_{\rm UV}$ has to be sufficiently negative in order for z to be bounded. For spin 1, z can be bounded for small positive $\bar{\alpha}_{\rm UV}$.

As an example, we may consider the specific case where $\bar{\alpha}_{\rm UV}$ is negligible, setting $\bar{\alpha}_{\rm UV}=0$. For spin $\frac{1}{2}$, we have $\bar{\alpha}_{\rm UV}=0\geq -\frac{1}{256}=\bar{\alpha}^*$, thus $\bar{\alpha}_{\rm IR}\geq 0,\ \forall\ z\in\mathbb{R}_+$, and hence z is unbounded. On the other hand, for spin 1, we have $\bar{\alpha}_{\rm UV}=0<\frac{23}{762}=\bar{\alpha}^*$, so that z is bounded on a region $[0,z_1]\cup[z_2,\infty)$, corresponding to the second case of (1b). In the spin-0 case, for any ξ , the $\bar{\alpha}_{\rm UV}$ coefficient has to be negative to produce a bound, therefore z is unbounded.

Our expressions from Table V reproduce the ones from [42] upon neglecting the \bar{c} coefficient and changing the convention for z. ¹⁸ Our conclusions for $\alpha_{\rm UV}=0$ differ from those in [42] due to the \bar{c} contribution—originating from the R^2 operator, which is not taken into account in [42]. As seen above, the \bar{c} contribution crucially favors positivity. The case studied in [42] is instead exactly recovered from our results by tuning $\bar{\alpha}_{\rm UV}+\bar{c}$ to zero.

¹⁸In [42], for d = 3, the convention $M = \frac{1}{2}$ is used and z is defined as $\frac{|q|}{m}$. This differs from our definition of z by a factor of $\sqrt{2}$.

TABLE VI. Reduced coefficient $\Delta \bar{\alpha}$, $\Delta \bar{\beta}$ in d = 4.

Spin	\Deltaar{lpha}	\Deltaar{eta}
0	$\frac{7z^4}{1440} - \frac{z^2}{180} + \frac{1}{120}\log\frac{M}{m}$	$\frac{z^4}{1440} - \frac{z^2}{180} + \frac{1}{120} \log \frac{M}{m}$
$\frac{1}{2}$	$\frac{z^4}{90} - \frac{11z^2}{360} + \frac{1}{40} \log \frac{M}{m}$	$\frac{7z^4}{360} - \frac{11z^2}{360} + \frac{1}{40}\log\frac{M}{m}$
1	$\frac{29z^4}{160} - \frac{31z^2}{60} + \frac{13}{120} \log \frac{M}{m}$	$\frac{27z^4}{160} - \frac{31z^2}{60} + \frac{13}{120}\log\frac{M}{m}$

TABLE VII. Condition for the existence of IR consistency bounds on the charge-to-mass ratio z in d = 4.

Spin	Condition for z bounded
0	$\bar{\alpha}_{\rm UV} < \frac{1}{630} - \frac{1}{120} \log \frac{M}{m} \text{ or } \bar{\beta}_{\rm UV} < \frac{1}{90} - \frac{1}{120} \log \frac{M}{m}$
$\frac{1}{2}$	$\bar{\alpha}_{\mathrm{UV}} < \frac{121}{5760} - \frac{1}{40} \log \frac{M}{m} \text{ or } \bar{\beta}_{\mathrm{UV}} < \frac{121}{10080} - \frac{1}{40} \log \frac{M}{m}$
1	$\bar{\alpha}_{\mathrm{UV}} < \frac{961}{2610} - \frac{13}{120} \log \frac{M}{m} \text{ or } \bar{\beta}_{\mathrm{UV}} < \frac{961}{2610} - \frac{13}{120} \log \frac{M}{m}$

2. Case d=4

The values of $\Delta \bar{\alpha}$, $\Delta \bar{\beta}$ are presented in Table VI. The scalar case is independent of ξ in d=4 due to the vanishing of the trace of the stress tensor; see (2.10). The \bar{c} coefficient originating from R^2 features a logarithm that corresponds to the effect of the 4d beta function shown in Tables I and II.

From Table VI we have that both \bar{a} and \bar{c} are positive and \bar{b} negative for any spin, for both $\Delta \bar{\alpha}$ and $\Delta \bar{\beta}$. We are thus in case (1b). A bound on z appears if $\bar{\alpha}_{UV}$ or $\bar{\beta}_{UV}$ is sufficiently negative, and the exact condition is given in Table VII. As an example, we may consider the specific case where $\bar{\alpha}_{UV}$, $\bar{\beta}_{UV}$ are negligible, setting $\bar{\alpha}_{UV} = 0$, $\bar{\beta}_{UV} = 0$. Assuming that $\frac{M}{m} \gtrsim 50$, z is unbounded for any spin.

Our results reproduces those from [42] for d=4 when ignoring the logarithmic term (i.e., \bar{c}) or absorbing it into $\bar{\alpha}_{\rm UV}$, $\bar{\beta}_{\rm UV}$ and changing the convention for z. Accordingly, the special case considered in [42] is exactly reproduced here by tuning $\bar{\alpha}_{\rm UV} + \bar{c} = 0$.

3. Case d=5

The values of $\Delta \bar{\alpha}$, $\Delta \bar{\beta}$ are presented in Table VIII. We have $\bar{a}>0$, $\bar{c}<0$ for all spins, for both $\Delta \bar{\alpha}$, $\Delta \bar{\beta}$ and any ξ . We have $\bar{b}<0$ for spin $\frac{1}{2}$ and 1, and for spin 0 we have $\bar{b}<0$ for $\Delta \bar{\beta}$ and $\mathrm{sign}(\bar{b})=\mathrm{sign}(3-5\xi)$ for $\Delta \bar{\alpha}$. We are thus in cases (1a) and (1b). A bound on z appears if \bar{a}_{UV} or $\bar{\beta}_{\mathrm{UV}}$ is sufficiently small, and the exact condition is given in Table IX.

As an example, we may consider the specific case where $\bar{\alpha}_{\rm UV}$, $\bar{\beta}_{\rm UV}$ are negligible, setting $\bar{\alpha}_{\rm UV}=0$, $\bar{\beta}_{\rm UV}=0$. We obtain WGC-like bounds for all spins, as shown in

TABLE VIII. Reduced coefficients $\Delta \bar{\alpha}$ and $\Delta \bar{\beta}$ in d = 5.

Spin	\Deltaar{lpha}	\Deltaar{eta}
0	$\frac{7z^4}{2880} - \frac{(3-5\xi)z^2}{360} - \frac{60\xi^2 - 20\xi + 23}{2160}$	$\frac{z^4}{2880} - \frac{z^2}{216} - \frac{1}{120}$
$\frac{1}{2}$	$\frac{z^4}{180} - \frac{7z^2}{180} - \frac{4}{135}$	$\frac{7z^4}{720} - \frac{7z^2}{216} - \frac{1}{40}$
1	$\frac{67z^4}{720} - \frac{197z^2}{360} - \frac{151}{1080}$	$\frac{61z^4}{720} - \frac{25z^2}{54} - \frac{7}{60}$

TABLE IX. Condition for the existence of IR consistency bounds on the charge-to-mass ratio z and IR consistency bounds on z if $\bar{\alpha}_{\rm UV} = \bar{\beta}_{\rm UV} = 0$ in d = 5.

Spin	Condition for z bounded	Bound if $\bar{\alpha}_{UV} = 0$	_
0	$\bar{\alpha}_{\text{UV}} < \begin{cases} \frac{60\xi^2 - 20\xi + 23}{2160} & \text{if } \xi \ge \frac{3}{5} \\ \frac{720\xi^2 - 500\xi + 269}{15120} & \text{if } \xi < \frac{3}{5} \\ \text{or } \bar{\beta}_{\text{UV}} < \frac{77}{3740} \end{cases}$	Fig. 1	$z \ge 3.87$
$\frac{1}{2}$	$\bar{\alpha}_{\rm UV} < \frac{211}{2160} \text{ or } \bar{\beta}_{\rm UV} < \frac{337}{6480}$	$z \ge 2.77$	$z \ge 1.99$
1	$\bar{\alpha}_{\rm UV} < \frac{136661}{144720} \text{ or } \bar{\beta}_{\rm UV} < \frac{74029}{98820}$	$z \ge 2.48$	$z \ge 2.39$

Table XXIX. In the spin-0 case, the bound is ξ -dependent. Positivity excludes a region in the $z\xi$ -plane, as shown in Fig. 1. For reference, we include in Fig. 1 and in analogous figures in higher dimensions the value of ξ for which the scalar is conformally coupled if $m \to 0$. The allowed region in Fig. 1 has a critical point to the left, which imposes a lower bound on the charge-to-mass ratio for all ξ . The subsequent WGC bound for all ξ is $z \ge \sqrt{\frac{13+\sqrt{937}}{18}} \approx 1.56$.

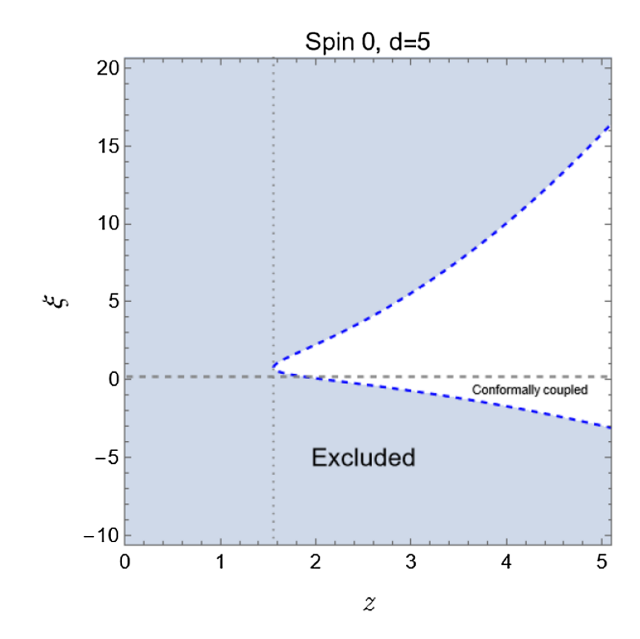


FIG. 1. Infrared consistency bounds on the charged spin 0 particle in d = 5.

¹⁹In [42], for d = 4, the convention $M^2 = \frac{1}{2}$ is used. Hence, the definition of z differs from ours by a factor of 2.

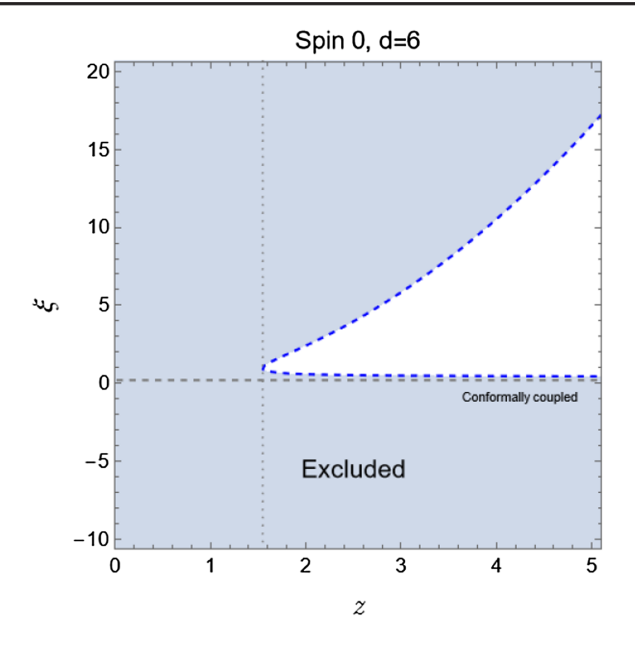


FIG. 2. Infrared consistency bounds on the charged spin 0 particle in the regime $\log \frac{M}{m} \gg 1$ (here with $\log \frac{M}{m} = 100$) in d = 6.

4. Case d=6

The values of $\Delta \bar{\alpha}$, $\Delta \bar{\beta}$ are presented in Table X. The \bar{b} and \bar{c} coefficients originating, respectively, from F^2R and R^2 feature a logarithm that corresponds to the effect of the 6d beta function from Tables I and II. This logarithm will in turn influence the WGC-like bounds, as discussed below.

From Table X, we have $\bar{a} > 0$, $\bar{c} < 0$ for all spins, for both $\Delta \bar{a}$, $\Delta \bar{\beta}$ and any ξ . We have $\bar{b} < 0$ for spin $\frac{1}{2}$ and 1, and for spin 0 we have $\bar{b} < 0$ for $\Delta \bar{\beta}$ and sign(\bar{b}) = sign($50\xi - 23$) for $\Delta \bar{a}$. We are thus in cases (1a) and (1b).

TABLE XII. IR consistency bounds on z if $\bar{\alpha}_{UV} = \bar{\beta}_{UV} = 0$ and $\log \frac{M}{m} \gg 1$ in d = 6.

Spin	Bound if $\bar{\alpha}_{UV} = 0$	Bound if $\bar{\beta}_{\mathrm{UV}} = 0$
0	Fig. 2	$z \ge 3.46\sqrt{\log \frac{M}{m}}$
$\frac{1}{2}$	$z \ge 2.79 \sqrt{\log \frac{M}{m}}$	$z \ge 1.85 \sqrt{\log \frac{M}{m}}$
1	$z \ge 2.42\sqrt{\log\frac{M}{m}}$	$z \ge 2.27 \sqrt{\log \frac{M}{m}}$

A bound on z appears if $\bar{\alpha}_{\rm UV}$ or $\bar{\beta}_{\rm UV}$ is sufficiently small, and the exact condition is given in Table XI.

As an example, we may consider the specific case where $\bar{\alpha}_{\rm UV}$, $\bar{\beta}_{\rm UV}$ is negligible, setting $\bar{\alpha}_{\rm UV}=0$, $\bar{\beta}_{\rm UV}=0$. We obtain WGC-like bounds for all spins, that depend on $\log \frac{M}{m}$. We focus on the regime where $\log \frac{M}{m} \gg 1$, and the results are shown in Table XII. The bounds presented are weaker than those obtained for small $\log \frac{M}{m}$ and thus hold for any value of $\frac{M}{m}$.

We emphasize that the logarithmic enhancement occurring in the bounds is tied to the positive sign of the 6d beta functions. While the positive beta functions lead to stronger bounds on z at large $\log \frac{M}{m}$, negative beta functions would lead to weaker bounds on z, that are independent of the logarithm.

In the spin-0 case, the ξ -dependent bound is shown in Fig. 2, where $\log \frac{M}{m}$ was set to 100 to plot the exclusion region. The allowed region in Fig. 2 has a critical point to the left which imposes a lower bound for the charge-to-mass ratio for all ξ . This critical lower bound increases with $\log \frac{M}{m}$, converging to the limit $\sqrt{\frac{880+5\sqrt{93410}}{1007}} \approx 1.55$. For

TABLE X. Reduced coefficients $\Delta \bar{\alpha}$ and $\Delta \bar{\beta}$ in d = 6.

Spin	\Deltaar{lpha}	\Deltaar{eta}
0	$\frac{7z^4}{1440} - \left(\frac{(23 - 50\xi)z^2}{1200} + \frac{15\xi^2 - 5\xi + 3}{240}\right) \log \frac{M}{m}$	$\frac{z^4}{1440} - \left(\frac{z^2}{120} + \frac{1}{120}\right) \log \frac{M}{m}$
$\frac{1}{2}$	$\frac{z^4}{45} - \left(\frac{13z^2}{75} + \frac{31}{480}\right) \log \frac{M}{m}$	$\frac{7z^4}{180} - \left(\frac{2z^2}{15} + \frac{1}{20}\right) \log \frac{M}{m}$
1	$\frac{55z^4}{288} - \left(\frac{269z^2}{240} + \frac{1}{6}\right) \log \frac{M}{m}$	$\frac{49z^4}{288} - \left(\frac{7z^2}{8} + \frac{1}{8}\right) \log \frac{M}{m}$

TABLE XI. Conditions for the existence of bounds on z in d = 6.

Spin	Condition for z bounded	
0	$\begin{cases} \bar{\alpha}_{\rm UV} < \frac{15\xi^2 - 5\xi + 3}{240} \log \frac{M}{m} & \text{if } \xi > \frac{23}{50} \\ \bar{\alpha}_{\rm UV} < \left(\frac{15\xi^2 - 5\xi + 3}{240} + \frac{(23 - 50\xi)^2}{28000} \log \frac{M}{m}\right) \log \frac{M}{m} & \text{if } \xi \leq \frac{23}{50} \end{cases} \text{ or } \bar{\beta}_{\rm UV} < \left(\frac{1}{120} + \frac{1}{40} \log \frac{M}{m}\right) \log \frac{M}{m}$	
$\frac{1}{2}$	$\bar{\alpha}_{\mathrm{UV}} < \left(\frac{31}{480} + \frac{169}{500}\log\frac{M}{m}\right)\log\frac{M}{m} \text{ or } \bar{\beta}_{\mathrm{UV}} < \left(\frac{1}{20} + \frac{4}{35}\log\frac{M}{m}\right)\log\frac{M}{m}$	
1	$\bar{\alpha}_{\mathrm{UV}} < \left(\frac{1}{6} + \frac{72361}{44000} \log \frac{M}{m}\right) \log \frac{M}{m} \text{ or } \bar{\beta}_{\mathrm{UV}} < \left(\frac{1}{8} + \frac{9}{8} \log \frac{M}{m}\right) \log \frac{M}{m}$	

smaller $\log \frac{M}{m}$, the bound is only slightly weaker, with, e.g., $z \ge 1.27$ if $\log \frac{M}{m} = 1$, which holds for any $\log \frac{M}{m} \ge 1$ and any ξ . Finally, if $\xi \le \frac{23}{50}$, the WGC-like bound strengthens to $z \ge \sqrt{\frac{6(23-50\xi)}{35}\log \frac{M}{m}}$, which holds for any value of $\frac{M}{m}$, analogous to other bounds in Table XII.

5. Case d = 7

The values of $\Delta \bar{\alpha}$, $\Delta \bar{\beta}$ are presented in Table XIII. We have $\bar{a}>0$, $\bar{c}>0$ for all spins, for both $\Delta \bar{\alpha}$, $\Delta \bar{\beta}$ and any ξ . We have $\bar{b}>0$ for spin $\frac{1}{2}$ and 1, and for spin 0 we have $\bar{b}>0$ for $\Delta \bar{\beta}$ and $\mathrm{sign}(\bar{b})=\mathrm{sign}(37-90\xi)$ for $\Delta \bar{\alpha}$. We are thus in cases (1a) and (1b). A bound on z appears if $\bar{\alpha}_{\mathrm{UV}}$ or $\bar{\beta}_{\mathrm{UV}}$ is sufficiently small, and the exact condition is given in Table XIV.

As an example, we consider the specific case $\bar{\alpha}_{UV}=0$, $\bar{\beta}_{UV}=0$. For spin $\frac{1}{2}$, we are in case (1a) with $\bar{\alpha}^*>0$, hence z is unbounded. For spin 1, we are in case (1b) with $-\bar{\alpha}^*>0$. As a result, z is bounded to two disjoint regions, with the one at larger z being WGC-like. For spin 0, the $\Delta\bar{\beta}$ does not constrain z, while a ξ -dependent bound exists from $\Delta\bar{\alpha}$. This is shown in Fig. 3.

This region in Fig. 3 has critical points on the left and bottom. If $z \leq \sqrt{\frac{11+\sqrt{257}}{10}} \approx 1.64$, then $\bar{\alpha}_{\rm IR} \geq 0$, $\forall \ \xi$; and if $\xi \leq \frac{225+\sqrt{26985}}{360} \approx 1.08$, then $\bar{\alpha}_{\rm IR} \geq 0$, $\forall \ z$. Conversely, when $\xi > 1.08$, the domain of z is restricted to two disjoint regions, corresponding to the $-\bar{c} \leq \bar{\alpha}_{\rm UV} < -\bar{\alpha}^*$ case in (1b). The domain at larger z is WGC-like.

TABLE XIII. Reduced coefficients $\Delta \bar{\alpha}$ and $\Delta \bar{\beta}$ in d = 7.

Spin	\Deltaar{lpha}	\Deltaar{eta}
0	$\frac{7z^4}{1440} + \frac{(37 - 90\xi)z^2}{1800} + \frac{540\xi^2 - 180\xi + 83}{9000}$	$\frac{z^4}{1440} + \frac{7z^2}{900} + \frac{1}{180}$
$\frac{1}{2}$	$\frac{z^4}{45} + \frac{83z^2}{450} + \frac{17}{375}$	$\frac{7z^4}{180} + \frac{61z^2}{450} + \frac{1}{30}$
1	$\frac{47z^4}{240} + \frac{57z^2}{50} + \frac{287}{2250}$	$\frac{41z^4}{240} + \frac{127z^2}{150} + \frac{4}{45}$

TABLE XIV. Condition for the existence of IR consistency bounds on the charge-to-mass ratio z and IR consistency bounds on z if $\bar{\alpha}_{\rm UV} = \bar{\beta}_{\rm UV} = 0$ in d = 7.

Spin	Condition for z bounded	Bound if $\bar{\alpha}_{UV} = 0$	Bound if $\bar{\beta}_{\rm UV} = 0$
0	$\bar{\alpha}_{\mathrm{UV}} < \begin{cases} \frac{-\frac{540\xi^2 - 180\xi + 83}{9000}}{\frac{1080\xi^2 - 1350\xi + 197}{15750}} & \text{if } \xi \leq \frac{37}{90} \\ \frac{15750}{\text{or } \bar{\beta}_{\mathrm{UV}}} < -\frac{1}{180} \end{cases}$	Fig. 3	Unbounded
$\frac{1}{2}$	$\bar{\alpha}_{\mathrm{UV}} < -\frac{17}{375} \text{ or } \bar{\beta}_{\mathrm{UV}} < -\frac{1}{30}$	Unbounded	Unbounded
1	$\bar{\alpha}_{\mathrm{UV}} < -\frac{287}{2250} \text{ or } \bar{\beta}_{\mathrm{UV}} < -\frac{4}{45}$	Unbounded	Unbounded

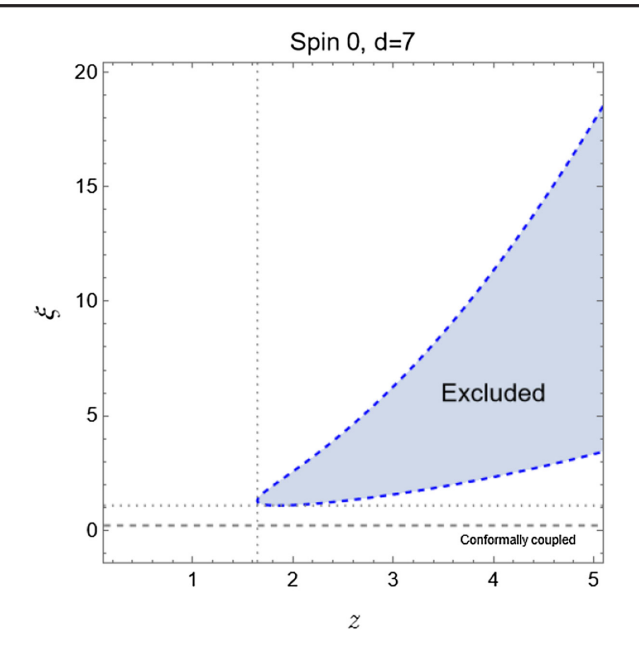


FIG. 3. Infrared consistency bounds on the charged spin 0 particle in d = 7.

6. Case d = 8

The values of $\Delta \bar{\alpha}$, $\Delta \bar{\beta}$ are presented in Table XV. All coefficients feature a logarithm corresponding to the effect of the 8d beta function shown in Tables I and II.

From Table XV, we have $\bar{a} > 0$ and $\bar{c} > 0$ in all cases. We have $\bar{b} < 0$ for spin 1 for both $\Delta \bar{\alpha}$ and $\Delta \bar{\beta}$, and $\bar{b} > 0$ for both spin $\frac{1}{2}$ and 0 for $\Delta \bar{\beta}$, while for $\Delta \bar{\alpha}$ we have $\bar{b} > 0$ for

TABLE XV. Reduced coefficients $\Delta \bar{\alpha}$ and $\Delta \bar{\beta}$ in d = 8.

Spin	\Deltaar{lpha}	\Deltaar{eta}
0	$\left(\frac{7z^4}{720} + \frac{(27 - 70\xi)z^2}{1260} + \frac{15\xi^2 - 5\xi + 2}{270}\right) \log \frac{M}{m}$	$\left(\frac{z^4}{720} + \frac{z^2}{135} + \frac{1}{240}\right) \log \frac{M}{m}$
$\frac{1}{2}$	$\left(\frac{4z^4}{45} + \frac{121z^2}{315} + \frac{19}{270}\right) \log \frac{M}{m}$	$\left(\frac{7z^4}{45} + \frac{37z^2}{135} + \frac{1}{20}\right) \log \frac{M}{m}$
1	$\left(\frac{289z^4}{720} + \frac{1459z^2}{1260} + \frac{29}{270}\right)\log\frac{M}{m}$	$\left(\frac{247z^4}{720} + \frac{112z^2}{135} + \frac{17}{240}\right)\log\frac{M}{m}$

TABLE XVI. Condition for the existence of IR consistency bounds on the charge-to-mass ratio z and IR consistency bounds on z if $\bar{\alpha}_{\rm UV} = \bar{\beta}_{\rm UV} = 0$ in d=8.

Spin	Condition for z bounded	Bound if $\bar{\alpha}_{UV} = 0$	Bound if $\bar{\beta}_{\rm UV} = 0$
0	$\begin{split} \bar{\alpha}_{\text{UV}} < \log \frac{M}{m} \begin{cases} -\frac{15\xi^2 - 5\xi + 2}{270} & \text{if } \xi \leq \frac{27}{70} \\ \frac{882\xi^2 - 1582\xi + 163}{37044} & \text{if } \xi > \frac{27}{70} \\ \text{or } \bar{\beta}_{\text{UV}} < -\frac{1}{240} \log \frac{M}{m} \end{split}$	Fig. 4	Unbounded
$\frac{1}{2}$	$\bar{\alpha}_{\mathrm{UV}} < -\frac{19}{270} \log \frac{M}{m} \text{ or } \bar{\beta}_{\mathrm{UV}} < -\frac{1}{20} \log \frac{M}{m}$	Unbounded	Unbounded
1	$\bar{\alpha}_{\mathrm{UV}} < -\frac{29}{270} \log \frac{M}{m} \text{ or } \bar{\beta}_{\mathrm{UV}} < -\frac{17}{240} \log \frac{M}{m}$	Unbounded	Unbounded

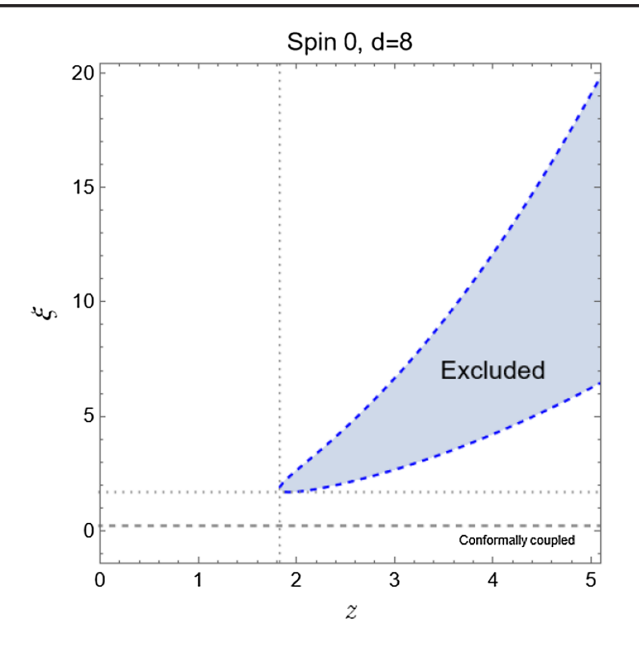


FIG. 4. Infrared consistency bounds on the charged spin 0 particle in d = 8.

spin $\frac{1}{2}$ and sign(\bar{b}) = sign($70\xi-27$) for spin 0. We are thus in cases (1a) and (1b). A bound on z appears if $\bar{\alpha}_{\rm UV}$ or $\bar{\beta}_{\rm UV}$ are sufficiently small, the exact condition is given in Table XVI.

As an example, we consider the specific case $\bar{\alpha}_{\rm UV}=0$, $\bar{\beta}_{\rm UV}=0$. For spin $\frac{1}{2}$ and 1, we are in case (1a) for both $\Delta\bar{\alpha}$ and $\Delta\bar{\beta}$; hence, z is unbounded. For spin 0, $\Delta\bar{\beta}$ does not constrain z, while a ξ -dependent bound exists from $\Delta\bar{\alpha}$. It is shown in Fig. 4. The region in Fig. 4 has critical points to the left and bottom. If $z \leq \sqrt{\frac{92+5\sqrt{562}}{63}} \approx 1.83$, we have $\bar{\alpha}_{\rm IR}>0$, \forall ξ ; and if $\xi \leq \frac{113+\sqrt{9835}}{126} \approx 1.68$, we have $\bar{\alpha}_{\rm IR}>0$, \forall z. Conversely, when $\xi>1.68$, the domain of z is restricted to two disjoint regions, corresponding to the $-\bar{c} \leq \bar{\alpha}_{\rm UV} < -\bar{\alpha}^*$ case in (1b). The domain at larger z is WGC-like.

7. Case d = 9

The values of $\Delta\bar{\alpha}$, $\Delta\bar{\beta}$ are presented in Table XVII. We have $\bar{a}<0$, $\bar{c}<0$ for all spins, for both $\Delta\bar{\alpha}$, $\Delta\bar{\beta}$ and any ξ . We have $\bar{b}<0$ for spin $\frac{1}{2}$ and 1, and for spin 0 we have $\bar{b}>0$ for $\Delta\bar{\beta}$ and $\mathrm{sign}(\bar{b})=\mathrm{sign}(100\xi-37)$ for $\Delta\bar{\alpha}$. We are thus in cases (2a) and (2b). The positivity bounds are satisfied if $\bar{\alpha}_{\mathrm{UV}}$ and $\bar{\beta}_{\mathrm{UV}}$ are sufficiently large and for a finite range of z. That is, z always features an upper bound in d=9. The exact condition for having IR consistency for some z is given in Table XVIII.

As a first example, we consider the specific case $\bar{\alpha}_{\rm UV}=0$, $\bar{\beta}_{\rm UV}=0$. For spin $\frac{1}{2}$, 1 and for the $\Delta\bar{\beta}$ coefficient of spin 0, we are in case (2b) with $-\bar{\alpha}^*=-\bar{c}>0$; hence, these cases are fully excluded.

A second example is to consider $\bar{\alpha}_{\rm UV}, \bar{\beta}_{\rm UV} \gg 1$. In that case, for any spin, there is an upper bound on z. The bounds take the form $z < \bar{C}(\bar{\alpha}_{\rm UV}^{1/4}, \bar{\beta}_{\rm UV}^{1/4})$ with $\bar{C} = (-\bar{a})^{-1/4}$, and the exact values are given in Table XVIII. Translating to the nonreduced notation, we have the bound

$$g|q|m^{\frac{1}{4}} < C\alpha_{\text{UV}}^{1/4} \tag{B1}$$

with $C = \bar{C}K_9^{1/4}$, and similarly for $\beta_{\rm UV}$. This upper bound on g|q| is independent of the strength of gravity, depending only on the UV coefficient.

The bound (B1) may be compared to strong coupling estimates of EFT coefficients. Ignoring all loop factors for simplicity, we have $\alpha_{UV} \sim \Lambda^{-9}$, $m < \Lambda$, with Λ being the

TABLE XVII. Reduced coefficients $\Delta \bar{\alpha}$ and $\Delta \bar{\beta}$ in d = 9.

Spin	\Deltaar{lpha}	\Deltaar{eta}
0	$-\frac{7z^4}{720} - \frac{(37 - 100\xi)z^2}{2520} - \frac{1500\xi^2 - 500\xi + 183}{44100}$	$-\frac{z^4}{720} - \frac{z^2}{210} - \frac{1}{450}$
$\frac{1}{2}$	$-\frac{4z^4}{45} - \frac{83z^2}{315} - \frac{424}{11025}$	$-\frac{7z^4}{45} - \frac{58z^2}{315} - \frac{2}{75}$
1	$-\frac{37z^4}{90} - \frac{247z^2}{315} - \frac{1397}{22050}$	$-\frac{31z^4}{90} - \frac{172z^2}{315} - \frac{1}{25}$

TABLE XVIII. Condition to have IR consistency for some z and IR consistency bounds on z if $\bar{\alpha}_{UV} = \bar{\beta}_{UV} = 0$ or $\bar{\alpha}_{UV}, \bar{\beta}_{UV} \gg 1$ in d = 9.

Spin	Necessary condition for IR consistency	Bound if $ar{lpha}_{\mathrm{UV}} = ar{eta}_{\mathrm{UV}} = 0$	Bound if $\bar{\alpha}_{\rm UV}, \bar{\beta}_{\rm UV} \gg 1$
0	$\bar{\alpha}_{\mathrm{UV}} \geq \begin{cases} -\frac{8000\xi^2 - 23000\xi + 1721}{1234800} & \text{if } \xi \geq \frac{37}{100} \\ \frac{1500\xi^2 - 500\xi + 183}{44100} & \text{if } \xi < \frac{37}{100} \\ \text{or } \bar{\beta}_{\mathrm{UV}} \geq \frac{1}{450} \end{cases}$	Excluded	$z \le 3.18\bar{\alpha}_{\rm UV}^{1/4}$ $z \le 5.18\bar{\beta}_{\rm UV}^{1/4}$
$\frac{1}{2}$	$\bar{\alpha}_{\mathrm{UV}} \geq \frac{424}{11025} \text{ or } \bar{\beta}_{\mathrm{UV}} \geq \frac{2}{75}$	Excluded	$z \le 1.83\bar{\alpha}_{\mathrm{UV}}^{1/4}$ $z \le 1.59\bar{\beta}_{\mathrm{UV}}^{1/4}$
1	$\bar{\alpha}_{\mathrm{UV}} \geq \frac{1397}{22050} \text{ or } \bar{\beta}_{\mathrm{UV}} \geq \frac{1}{25}$	Excluded	$z \le 1.25\bar{\alpha}_{\rm UV}^{1/4} z \le 1.31\bar{\beta}_{\rm UV}^{1/4}$

TABLE XIX. Reduced coefficients $\Delta \bar{\alpha}$ and $\Delta \bar{\beta}$ in d = 10.

Spin	\Deltaar{lpha}	\Deltaar{eta}
0	$-\left(\frac{7z^4}{720} + \frac{(97 - 270\xi)z^2}{8640} + \frac{270\xi^2 - 90\xi + 31}{11520}\right)\log\frac{M}{m}$	$-\left(\frac{z^4}{720} + \frac{z^2}{288} + \frac{1}{720}\right) \log \frac{M}{m}$
$\frac{1}{2}$	$-\left(\frac{8z^4}{45} + \frac{109z^2}{270} + \frac{47}{960}\right)\log\frac{M}{m}$	$-\left(\frac{14z^4}{45} + \frac{5z^2}{18} + \frac{1}{30}\right)\log\frac{M}{m}$
1	$-\left(\frac{101}{240} + \frac{1721z^2}{2880} + \frac{499}{11520}\right)\log\frac{M}{m}$	$-\left(\frac{83z^4}{240} + \frac{13z^2}{32} + \frac{19}{720}\right)\log\frac{M}{m}$

TABLE XX. Condition to have IR consistency for some z and IR consistency bounds on z if $\bar{\alpha}_{\rm UV} = \bar{\beta}_{\rm UV} = 0$ or $\bar{\alpha}_{\rm UV}, \bar{\beta}_{\rm UV} \gg 1$ in d=10.

Spin	Necessary condition for IR consistency	Bound if $ar{lpha}_{ m UV}=ar{eta}_{ m UV}=0$	Bound if $\bar{\alpha}_{\rm UV}, \bar{\beta}_{\rm UV} \gg 1$
0	$\bar{\alpha}_{\rm UV} \ge \log \frac{M}{m} \begin{cases} -\frac{4860\xi^2 - 29700\xi + 1597}{2903040} & \text{if } \xi > \frac{97}{270} \\ \frac{270\xi^2 - 90\xi + 31}{11520} & \text{if } \xi \le \frac{97}{270} \end{cases}$	Excluded	$z \le \left(\frac{720}{7\log_{m}^{M}}\bar{\alpha}_{\mathrm{UV}}\right)^{\frac{1}{4}}$ $z \le \left(\frac{720}{\log_{m}^{M}}\bar{\beta}_{\mathrm{UV}}\right)^{\frac{1}{4}}$
$\frac{1}{2}$	or $\bar{\beta}_{\text{UV}} \ge \frac{1}{720} \log \frac{M}{m}$ $\bar{\alpha}_{\text{UV}} \ge \frac{47}{960} \log \frac{M}{m} \text{ or } \bar{\beta}_{\text{UV}} \ge \frac{1}{30} \log \frac{M}{m}$	Excluded	$z \le \left(\frac{45}{8 \log_{m}^{M}} \bar{\alpha}_{\mathrm{UV}}\right)^{\frac{1}{4}}$
1	$\bar{\alpha}_{\rm UV} \ge \frac{499}{11520} \log \frac{M}{m} \text{ or } \bar{\beta}_{\rm UV} \ge \frac{19}{720} \log \frac{M}{m}$	Excluded	$z \le \left(\frac{45}{14 \log \frac{1}{M}} \bar{\beta}_{UV}\right)^{\frac{1}{4}}$ $z \le \left(\frac{720}{293 \log \frac{1}{M}} \bar{\alpha}_{UV}\right)^{\frac{1}{4}}$
			$z \le \left(\frac{240}{83 \log \frac{M}{m}} \bar{\beta}_{\rm UV}\right)^{\frac{1}{4}}$

EFT cutoff. The bound (B1) is *less* constraining than the strong coupling estimate $g|q|\sim \Lambda^{-5/2}$ except if $m\sim \Lambda$. Conversely, in a weakly coupled UV completion, with, e.g., $\alpha_{\rm UV}\sim \frac{\lambda}{\Lambda^9},\ \lambda\ll 1$, the bound (B1) can easily be constraining—while maintaining the assumption $\bar{\alpha}_{\rm UV}\gg 1$, i.e., $\alpha_{\rm UV}\gg \frac{m^5}{M^{14}}$.

8. Case d = 10

The values of $\Delta \bar{\alpha}$, $\Delta \bar{\beta}$ are presented in Table XIX. All coefficients feature a logarithm. The sign pattern is exactly the same as that for d=9. As a result, similar conclusions follow: IR consistency is satisfied if $\bar{\alpha}_{\rm UV}$ and $\bar{\beta}_{\rm UV}$ are large enough; see Table XX. Moreover, z is always bounded from above, as exemplified in Table XX. Translating to the nonreduced notation, we obtain the upper bound

$$g|q|m^{\frac{1}{2}} < C\alpha_{\mathrm{UV}}^{1/4} \tag{B2}$$

with $C = \bar{C} K_{10}^{1/4}$ and similarly for $\beta_{\rm UV}$.

9. Case d = 11

The values of $\Delta \bar{\alpha}$, $\Delta \bar{\beta}$ are presented in Table XXI. We have $\bar{a} > 0$, $\bar{c} > 0$ for all spins, for both $\Delta \bar{\alpha}$, $\Delta \bar{\beta}$ and any ξ . We have $\bar{b} > 0$ for spin $\frac{1}{2}$ and 1, and for spin 0 we have

 $\bar{b}>0$ for $\Delta\bar{\beta}$ and $\mathrm{sign}(\bar{b})=\mathrm{sign}(123-350\xi)$ for $\Delta\bar{\alpha}$. We are thus in cases (1a) and (1b). A bound on z appears if $\bar{\alpha}_{\mathrm{UV}}$ or $\bar{\beta}_{\mathrm{UV}}$ is sufficiently small, and the exact condition is given in Table XXII. The sign pattern is similar to d=7.

TABLE XXI. Reduced coefficients $\Delta \bar{\alpha}$ and $\Delta \bar{\beta}$ in d=11.

Spin	\Deltaar{lpha}	\Deltaar{eta}
0	$\frac{7z^4}{1080} + \frac{(123 - 350\xi)z^2}{20250} + \frac{2940\xi^2 - 980\xi + 323}{255150}$	$\frac{z^4}{1080} + \frac{11z^2}{6075} + \frac{1}{1575}$
$\frac{1}{2}$	$\frac{16z^4}{135} + \frac{2216z^2}{10125} + \frac{2896}{127575}$	$\frac{28z^4}{135} + \frac{904z^2}{6075} + \frac{8}{525}$
1	$\frac{31z^4}{108} + \frac{656z^2}{2025} + \frac{548}{25515}$	$\frac{25z^4}{108} + \frac{262z^2}{1215} + \frac{4}{315}$

TABLE XXII. Condition for the existence of IR consistency bounds on the charge-to-mass ratio z and IR consistency bounds on z if $\bar{\alpha}_{\rm UV} = \bar{\beta}_{\rm UV} = 0$ in d=11.

Spin	Condition for z bounded	Bound if $\bar{\alpha}_{UV} = 0$	Bound if $\bar{\beta}_{UV} = 0$
0	$\bar{\alpha}_{\text{UV}} < \begin{cases} -\frac{2940\xi^2 - 980\xi + 323}{255150} & \text{if } \xi \leq \frac{123}{350} \\ -\frac{9700\xi - 338}{2278125} & \text{if } \xi > \frac{123}{350} \\ \text{or } \bar{\beta}_{\text{UV}} < -\frac{1}{1575} \end{cases}$	Unbounded	Unbounded
$\frac{1}{2}$	$\bar{\alpha}_{ m UV} < -rac{2896}{127575} \ { m or} \ ar{eta}_{ m UV} < -rac{8}{525}$	Unbounded	Unbounded
1	$\bar{\alpha}_{\mathrm{UV}} < -\frac{548}{25515}$ or $\bar{\beta}_{\mathrm{UV}} < -\frac{4}{315}$	Unbounded	Unbounded

Consider the specific case $\bar{\alpha}_{\rm UV} = \bar{\beta}_{\rm UV} = 0$. For spin $\frac{1}{2}$ and 1, we are in case (1a) with $\bar{\alpha}^* > 0$; hence, z is unbounded. For spin 0, $\Delta \bar{\beta}$ does not constrain z, while a ξ -dependent bound would be expected from $\Delta \bar{\alpha}$. However, as in d=3, for every ξ , the coefficient $\bar{\alpha}_{\rm UV}$ must be negative 20 to generate a bound on z; hence, z is unbounded in this case.

APPENDIX C: DETAILED BOUNDS FROM EXTREMAL BLACK HOLES

We present the results from extremal black hole decay for each spacetime dimension. The discussion follows the same structure as that in Appendix B and does not need to be repeated.

1. Coefficients

Translating Eq. (B.15) of [27] to our operator basis and conventions, we obtain the $C_{\rm IR}$ coefficient:

$$C_{\rm IR} = \alpha_1 + \frac{\alpha_2}{2} + \frac{(d-4)^2 \alpha_3 + (2d^2 - 11d + 16)\alpha_4}{4(d-2)^2} + \frac{(2d^3 - 16d^2 + 45d - 44)\alpha_5}{2(d-3)(d-2)^2} + \frac{(d-4)\alpha_6 + (d-3)(\alpha_7 + \alpha_8)}{2(d-2)}.$$
 (C1)

Using the formalism of Sec. III A, we have $C_{\rm IR} = C_{\rm UV} + \Delta C$, where the correction ΔC produced by charged particles takes the form

$$\begin{split} \Delta C^{(s)} &= \frac{1}{(4\pi)^{d/2}} \left[\frac{g^4 q^4}{m^{8-d}} \Gamma \left(4 - \frac{d}{2} \right) a_C^{(s)} \right. \\ &+ \frac{g^2 q^2}{m^{6-d} M^{d-2}} \Gamma \left(3 - \frac{d}{2} \right) b_C^{(s)} \\ &+ \frac{1}{m^{4-d} M^{2d-4}} \Gamma \left(2 - \frac{d}{2} \right) c_C^{(s)} \right]. \end{split} \tag{C2}$$

The coefficients for each spin are

$$a_C^{(0)} = \frac{7}{1440}, \qquad b_C^{(0)} = \frac{(30\xi - 11)d - 120\xi + 38}{720(d - 2)},$$
 (C3a)

$$a_C^{(1/2)} = \frac{n}{360}, \qquad b_C^{(1/2)} = -\frac{n}{1440} \frac{19d - 52}{(d - 2)},$$
 (C3b)

$$a_C^{(1)} = \frac{7d + 233}{1440}, \qquad b_C^{(1)} = -\frac{11d^2 + 401d - 1162}{720(d - 2)}.$$
 (C3c)

$$c_C^{(0)} = \frac{1}{1440} \left[\frac{2(3-d)(2d^2 - 11d + 16)}{(d-3)(d-2)^2} + \frac{4(2d^3 - 16d^2 + 45d - 44)}{(d-3)(d-2)^2} + \frac{5(1-6\xi)^2(d-4)^2}{(d-2)^2} \right],$$
(C4a)

$$c_C^{(1/2)} = \frac{n}{11520} \frac{39d^3 - 305d^2 + 822d - 760}{(d-3)(d-2)^2},$$
 (C4b)

$$c_C^{(1)} = \frac{1}{1440} \frac{9d^4 + 86d^3 - 1073d^2 + 3118d - 2800}{(d-3)(d-2)^2}.$$
 (C4c)

2. Bounds

We apply the positivity analysis performed on the α and β coefficients in Sec. VI, but now on the C coefficient of the black hole charge-to-mass ratio. We present in Tables XXIII–XXX the results from d=4 to d=11,

TABLE XXIII. Reduced coefficient $\Delta \bar{C}$ in d = 4.

Spin	$\Delta ar{C}$
0	$\frac{7z^4}{1440} - \frac{z^2}{240} + \frac{1}{120}\log\frac{M}{m}$
$\frac{1}{2}$	$\frac{z^4}{90} - \frac{z^2}{30} + \frac{1}{40} \log \frac{M}{m}$
1	$\frac{29z^4}{160} - \frac{103z^2}{240} + \frac{13}{120}\log\frac{M}{m}$

TABLE XXIV. Reduced coefficient $\Delta \bar{C}$ and extremal black hole decay bounds on z if $\bar{C}_{\rm UV}=0$ in d=5.

Spin	$\Delta ar{C}$	Bound if $\bar{C}_{\mathrm{UV}} = 0$
0	$\frac{7z^4}{2880} - \frac{(17-30\xi)z^2}{2160} - \frac{12\xi^2 - 4\xi + 3}{432}$	Fig. 5
$\frac{1}{2}$	$\frac{z^4}{180} - \frac{43z^2}{1080} - \frac{5}{216}$	$z \ge 2.78$
1	$\frac{67z^4}{720} - \frac{559z^2}{1080} - \frac{13}{72}$	$z \ge 2.43$

TABLE XXV. Reduced coefficients $\Delta \bar{C}$ and extremal black hole decay bounds on z if $\bar{C}_{\rm UV}=0$ in d=6.

Spin	$\Delta ar{C}$	Bound if $\bar{C}_{\rm UV} = 0$
0	$\frac{7z^4}{1440} - \left(\frac{(7-15\xi)z^2}{360} + \frac{135\xi^2 - 45\xi + 16}{2160}\right) \log \frac{M}{m}$	Similar to Fig. 2
$\frac{1}{2}$	$\frac{z^4}{45} - \left(\frac{31z^2}{180} + \frac{101}{2160}\right) \log \frac{M}{m}$	$z \ge 2.78 \log \frac{M}{m}$
1	$\frac{55z^4}{288} - \left(\frac{41z^2}{36} + \frac{47}{216}\right) \log \frac{M}{m}$	$z \ge 2.44 \log \frac{M}{m}$

 $^{^{20}}$ Different from d=3, a curious cancellation of the ξ^2 term occurs in the condition for z bounded with $\xi>\frac{123}{350}$. Despite this cancellation, for any ξ in this domain, the $\Delta\bar{\alpha}$ coefficient has to be negative to produce a bound.

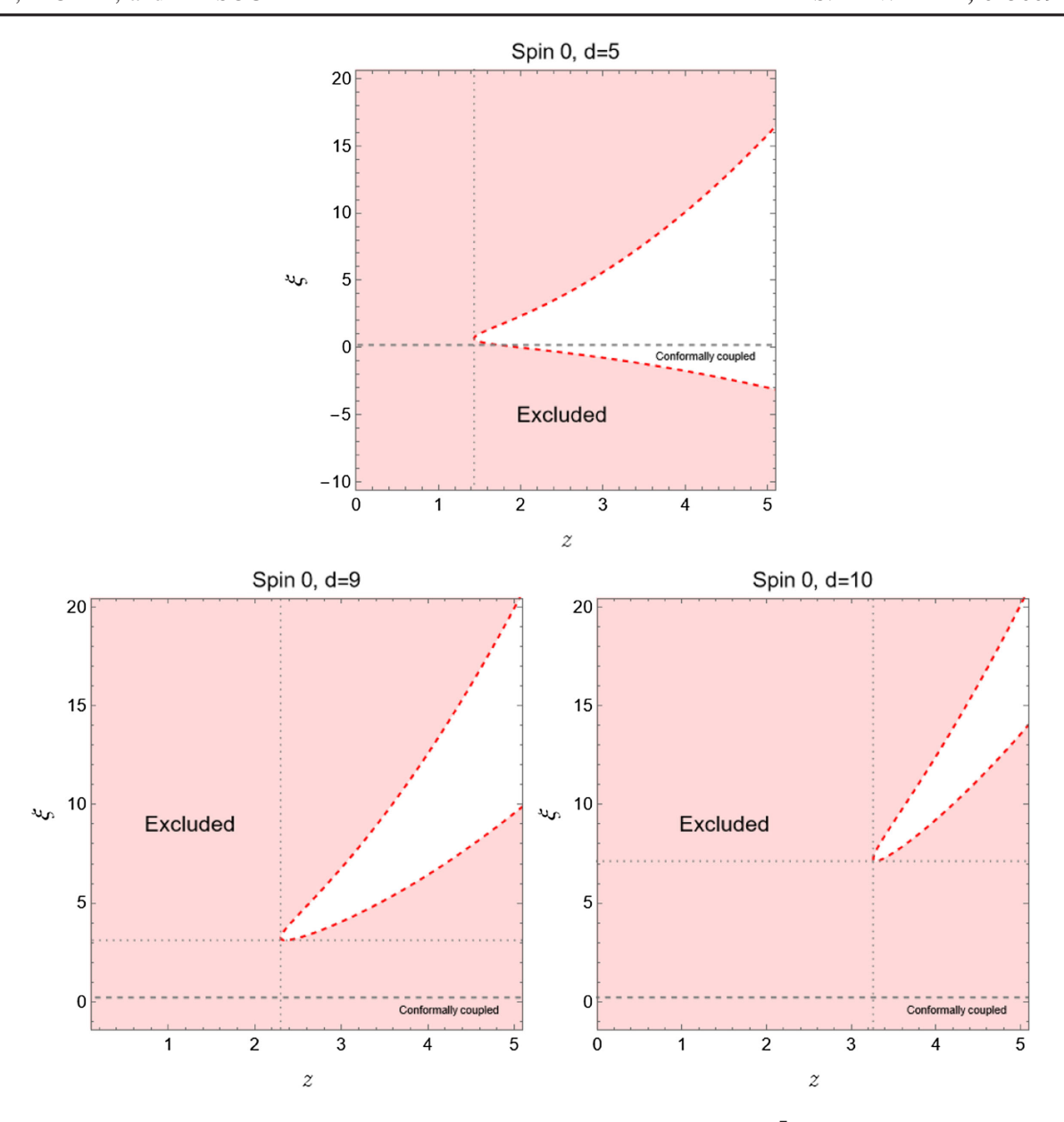


FIG. 5. Extremal black hole decay bounds on the charged spin 0 particle if $\bar{C}_{\rm UV}=0$ in $d=5,\,9,\,10$.

TABLE XXVI. Reduced coefficients $\Delta \bar{C}$ and extremal black hole decay bounds on z if $\bar{C}_{\rm UV}=0$ in d=7.

Spin	$\Delta ar{C}$	Bound if $\bar{C}_{\mathrm{UV}} = 0$
0	$\frac{7z^4}{1440} + \frac{(13-30\xi)z^2}{600} + \frac{45\xi^2 - 15\xi + 4}{750}$	Similar to Fig. 3
$\frac{1}{2}$	$\frac{z^4}{45} + \frac{9z^2}{50} + \frac{571}{18000}$	Unbounded
1	$\frac{47z^4}{240} + \frac{91z^2}{75} + \frac{1463}{9000}$	Unbounded

TABLE XXVII. Reduced coefficients $\Delta \bar{C}$ and extremal black hole decay bounds on z if $\bar{C}_{\rm UV}=0$ in d=8.

Spin	$\Delta ar{C}$	Bound if $\bar{C}_{\mathrm{UV}} = 0$
0	$\left(\frac{7z^4}{720} + \frac{(5-12\xi)z^2}{216} + \frac{300\xi^2 - 100\xi + 23}{5400}\right) \log \frac{M}{m}$	Similar to Fig. 4
$\frac{1}{2}$	$\left(\frac{4z^4}{45} + \frac{10z^2}{27} + \frac{29}{600}\right) \log \frac{M}{m}$	Unbounded
1	$\left(\frac{289z^4}{720} + \frac{275z^2}{216} + \frac{179}{1350}\right)\log\frac{M}{m}$	Unbounded

TABLE XXVIII. Reduced coefficients $\Delta \bar{C}$ and extremal black hole decay bounds on z if $\bar{C}_{\rm UV}=0$ and $\bar{C}_{\rm UV}\gg 1$ in d=9.

Spin	$\Delta ar{C}$	Bound if $\bar{C}_{\mathrm{UV}} = 0$	Bound if $\bar{C}_{\rm UV} \gg 1$
0	$-\frac{7z^4}{720} - \frac{(61 - 150\xi)z^2}{3780} - \frac{13500\xi^2 - 4500\xi + 947}{396900}$	Fig. 5	$z \le 3.18 \bar{C}_{\mathrm{UV}}^{1/4}$
$\frac{1}{2}$	$-\frac{4z^4}{45} - \frac{34z^2}{135} - \frac{2591}{99225}$	Excluded	$z \le 1.83 \bar{C}_{\mathrm{UV}}^{1/4}$
1	$-\frac{37z^4}{90} - \frac{1669z^2}{1890} - \frac{15023}{198450}$	Excluded	$z \le 1.25 \bar{C}_{\rm UV}^{1/4}$

TABLE XXIX. Reduced coefficients $\Delta \bar{C}$ and extremal black hole decay bounds on z if $\bar{C}_{\rm UV}=0$ in d=10.

Spin	$\Delta ar{C}$	Bound if $\bar{C}_{\rm UV} = 0$	Bound if $\bar{C}_{\rm UV} \gg 1$
0	$-\left(\frac{7z^4}{720} + \frac{(2-5\xi)z^2}{160} + \frac{378\xi^2 - 126\xi + 25}{16128}\right) \log \frac{M}{m}$	Fig. 5	$z \le \left(\frac{720}{7\log_m^M} \bar{C}_{\mathrm{UV}}\right)^{\frac{1}{4}}$
$\frac{1}{2}$	$-\left(\frac{8z^4}{45} + \frac{23z^2}{60} + \frac{19}{576}\right)\log\frac{M}{m}$	Excluded	$z \le \left(\frac{45}{8\log_{m}^{\underline{M}}}\bar{C}_{\mathrm{UV}}\right)^{\frac{1}{4}}$
1	$-\left(\frac{101z^4}{240} + \frac{329z^2}{480} + \frac{809}{16128}\right)\log\frac{M}{m}$	Excluded	$z \le \left(\frac{240}{101 \log_{m}^{\underline{M}}} \bar{C}_{\mathrm{UV}}\right)^{\frac{1}{4}}$

in the same format as those presented in Sec. VI for the analysis of amplitudes.

Finally, we present the exclusion region in the $z\xi$ -plane for d=5 to exemplify the similarity with the results from amplitude consistency; see Fig. 1. We also show the figures for d=9 and d=10, which were not presented before

TABLE XXX. Reduced coefficients $\Delta \bar{C}$ and extremal black hole decay bounds on z if $\bar{C}_{UV} = 0$ in d = 11.

Spin	$\Delta ar{C}$	Bound if $\bar{C}_{\mathrm{UV}} = 0$
0	$\frac{7z^4}{1080} + \frac{(83-210\xi)z^2}{12150} + \frac{5880\xi^2-1960\xi+373}{510300}$	Unbounded
$\frac{1}{2}$	$\frac{16z^4}{135} + \frac{1256z^2}{6075} + \frac{3881}{255150}$	Unbounded
1	$\frac{31z^4}{108} + \frac{458z^2}{1215} + \frac{493}{20412}$	Unbounded

because the $\bar{\alpha}_{\rm UV}=0$ condition was considered together with the $\bar{\beta}_{\rm UV}=0$, which is stronger.

APPENDIX D: THE HEAT KERNEL COEFFICIENTS

The general expressions for the coefficients appearing in (4.9) and (4.10) are [47,48]

$$\begin{split} b_0 &= I \\ b_2 &= \frac{1}{6}RI - X \\ b_4 &= \frac{1}{360} \left(12\Box R + 5R^2 - 2R_{\mu\nu}R^{\mu\nu} + 2R_{\mu\nu\rho\sigma}R^{\mu\nu\rho\sigma} \right) I \\ &- \frac{1}{6}\Box X - \frac{1}{6}RX + \frac{1}{2}X^2 + \frac{1}{12}\Omega_{\mu\nu}\Omega^{\mu\nu}, \end{split} \tag{D1}$$

$$b_{6} = \frac{1}{360} \left(8D_{\rho}\Omega_{\mu\nu}D^{\rho}\Omega^{\mu\nu} + 2D^{\mu}\Omega_{\mu\nu}D_{\rho}\Omega^{\rho\nu} + 12\Omega_{\mu\nu}\Box\Omega^{\mu\nu} - 12\Omega_{\mu\nu}\Omega^{\nu\rho}\Omega_{\rho}^{\ \mu} + 6R_{\mu\nu\rho\sigma}\Omega^{\mu\nu}\Omega^{\rho\sigma} - 4R_{\mu}^{\nu}\Omega^{\mu\rho}\Omega_{\nu\rho} + 5R\Omega_{\mu\nu}\Omega^{\mu\nu} - 6\Box^{2}X + 60X\Box X + 30D_{\mu}XD^{\mu}X - 60X^{3} - 30X\Omega_{\mu\nu}\Omega^{\mu\nu} - 10R\Box X - 4R_{\mu\nu}D^{\nu}D^{\mu}X - 12D_{\mu}RD^{\mu}X + 30XXR$$

$$-12X\Box R - 5XR^{2} + 2XR_{\mu\nu}R^{\mu\nu} - 2XR_{\mu\nu\rho\sigma}R^{\mu\nu\rho\sigma} \right) + \frac{1}{7!} \left(18\Box^{2}R + 17D_{\mu}RD^{\mu}R - 2D_{\rho}R_{\mu\nu}D^{\rho}R^{\mu\nu} - 4D_{\rho}R_{\mu\nu}D^{\mu}R^{\rho\nu} + 9D_{\rho}R_{\mu\nu\sigma\lambda}D^{\rho}R^{\mu\nu\sigma\lambda} + 28R\Box R - 8R_{\mu\nu}\Box R^{\mu\nu} + 24R_{\mu\nu}D_{\rho}D^{\nu}R^{\mu\rho} + 12R_{\mu\nu\sigma\lambda}\Box R^{\mu\nu\sigma\lambda} + 35/9R^{3} - 14/3RR_{\mu\nu}R^{\mu\nu} + 14/3RR_{\mu\nu\rho\sigma}R^{\mu\nu\rho\sigma} - 208/9R_{\mu\nu}R^{\mu\rho}R^{\rho} + 64/3R_{\mu\nu}R_{\rho\sigma}R^{\mu\rho\nu\sigma} - 16/3R^{\mu}_{\nu}R_{\mu\rho\sigma\lambda}R^{\nu\rho\sigma\lambda} + 44/9R^{\mu\nu}_{\alpha\beta}R_{\mu\nu\rho\sigma}R^{\rho\sigma\alpha\beta} + 80/9R_{\mu}^{\nu}{}_{\rho}^{\sigma}R^{\mu\alpha\rho\beta}R_{\nu\alpha\sigma\beta} \right) I \tag{D2}$$

with *I* being the identity matrix for internal indexes.

T. N. Pham and T. N. Truong, Evaluation of the derivative quartic terms of the meson chiral Lagrangian from forward dispersion relation, Phys. Rev. D 31, 3027 (1985).

^[2] B. Ananthanarayan, D. Toublan, and G. Wanders, Consistency of the chiral pion pion scattering amplitudes with axiomatic constraints, Phys. Rev. D **51**, 1093 (1995).

^[3] A. Adams, N. Arkani-Hamed, S. Dubovsky, A. Nicolis, and R. Rattazzi, Causality, analyticity and an IR obstruction to UV completion, J. High Energy Phys. 10 (2006) 014.

^[4] N. Arkani-Hamed, T.-C. Huang, and Y.-t. Huang, The EFT-Hedron, J. High Energy Phys. 05 (2021) 259.

- [5] L. Alberte, C. de Rham, S. Jaitly, and A. J. Tolley, Positivity bounds and the massless spin-2 pole, Phys. Rev. D 102, 125023 (2020).
- [6] L. Alberte, C. de Rham, S. Jaitly, and A. J. Tolley, QED positivity bounds, Phys. Rev. D 103, 125020 (2021).
- [7] J. Henriksson, B. McPeak, F. Russo, and A. Vichi, Rigorous bounds on light-by-light scattering, J. High Energy Phys. 06 (2022) 158.
- [8] J. Henriksson, B. McPeak, F. Russo, and A. Vichi, Bounding violations of the weak gravity conjecture, J. High Energy Phys. 08 (2022) 184.
- [9] B. Bellazzini, J. Elias Miró, R. Rattazzi, M. Riembau, and F. Riva, Positive moments for scattering amplitudes, Phys. Rev. D 104, 036006 (2021).
- [10] S. Caron-Huot, D. Mazac, L. Rastelli, and D. Simmons-Duffin, AdS bulk locality from sharp CFT bounds, arXiv:2106.10274.
- [11] B. Bellazzini, M. Riembau, and F. Riva, IR side of positivity bounds, Phys. Rev. D 106, 105008 (2022).
- [12] S. Caron-Huot and V. Van Duong, Extremal effective field theories, J. High Energy Phys. 05 (2021) 280.
- [13] S. Caron-Huot, D. Mazac, L. Rastelli, and D. Simmons-Duffin, Sharp boundaries for the swampland, J. High Energy Phys. 07 (2021) 110.
- [14] J. Davighi, S. Melville, and T. You, Natural selection rules: New positivity bounds for massive spinning particles, J. High Energy Phys. 02 (2022) 167.
- [15] C. de Rham, S. Melville, and J. Noller, Positivity bounds on dark energy: When matter matters, J. Cosmol. Astropart. Phys. 08 (2021) 018.
- [16] S. Caron-Huot, Y.-Z. Li, J. Parra-Martinez, and D. Simmons-Duffin, Causality constraints on corrections to Einstein gravity, J. High Energy Phys. 05 (2023) 122.
- [17] A. J. Tolley, Z.-Y. Wang, and S.-Y. Zhou, New positivity bounds from full crossing symmetry, J. High Energy Phys. 05 (2021) 255.
- [18] C. de Rham, A. J. Tolley, and J. Zhang, Causality constraints on gravitational effective field theories, Phys. Rev. Lett. 128, 131102 (2022).
- [19] C. de Rham, S. Kundu, M. Reece, A. J. Tolley, and S.-Y. Zhou, Snowmass white paper: UV constraints on IR physics, in *Snowmass* 2021 (2022), arXiv:2203.06805.
- [20] L.-Y. Chiang, Y.-t. Huang, L. Rodina, and H.-C. Weng, De-projecting the EFThedron, arXiv:2204.07140.
- [21] S. Caron-Huot, Y.-Z. Li, J. Parra-Martinez, and D. Simmons-Duffin, Graviton partial waves and causality in higher dimensions, Phys. Rev. D 108, 026007 (2023).
- [22] K. Häring, A. Hebbar, D. Karateev, M. Meineri, and J. a. Penedones, Bounds on photon scattering, arXiv:2211 .05795.
- [23] Y. Hamada, R. Kuramochi, G. J. Loges, and S. Nakajima, On (scalar QED) gravitational positivity bounds, arXiv: 2301.01999.
- [24] B. Bellazzini, G. Isabella, S. Ricossa, and F. Riva, Massive gravity is not positive, Phys. Rev. D **109**, 024051 (2024).
- [25] A. Eichhorn, A. O. Pedersen, and M. Schiffer, Application of positivity bounds in asymptotically safe gravity, arXiv:2405.08862.
- [26] B. Knorr and A. Platania, Unearthing the intersections: Positivity bounds, weak gravity conjecture, and asymptotic

- safety landscapes from photon-graviton flows, arXiv:2405 .08860.
- [27] Y. Kats, L. Motl, and M. Padi, Higher-order corrections to mass-charge relation of extremal black holes, J. High Energy Phys. 12 (2007) 068.
- [28] C. Cheung, J. Liu, and G. N. Remmen, Proof of the weak gravity conjecture from black hole entropy, J. High Energy Phys. 10 (2018) 004.
- [29] G. J. Loges, T. Noumi, and G. Shiu, Thermodynamics of 4D dilatonic black holes and the weak gravity conjecture, Phys. Rev. D **102**, 046010 (2020).
- [30] G. Goon and R. Penco, Universal relation between corrections to entropy and extremality, Phys. Rev. Lett. 124, 101103 (2020).
- [31] C. R. T. Jones and B. McPeak, The black hole weak gravity conjecture with multiple charges, J. High Energy Phys. 06 (2020) 140.
- [32] G. J. Loges, T. Noumi, and G. Shiu, Duality and supersymmetry constraints on the weak gravity conjecture, J. High Energy Phys. 11 (2020) 008.
- [33] N. Arkani-Hamed, Y.-t. Huang, J.-Y. Liu, and G. N. Remmen, Causality, unitarity, and the weak gravity conjecture, J. High Energy Phys. 03 (2022) 083.
- [34] Q.-H. Cao and D. Ueda, Entropy constraint on effective field theory, arXiv:2201.00931.
- [35] V. De Luca, J. Khoury, and S. S. C. Wong, Implications of the weak gravity conjecture for tidal Love numbers of black holes, arXiv:2211.14325.
- [36] N. Arkani-Hamed, L. Motl, A. Nicolis, and C. Vafa, The string landscape, black holes and gravity as the weakest force, J. High Energy Phys. 06 (2007) 060.
- [37] M. van Beest, J. Calderón-Infante, D. Mirfendereski, and I. Valenzuela, Lectures on the swampland program in string compactifications, Phys. Rep. **989**, 1 (2022).
- [38] M. Graña and A. Herráez, The swampland conjectures: A bridge from quantum gravity to particle physics, Universe 7, 273 (2021).
- [39] N. B. Agmon, A. Bedroya, M. J. Kang, and C. Vafa, Lectures on the string landscape and the swampland, arXiv:2212.06187.
- [40] C. Cheung and G. N. Remmen, Infrared consistency and the weak gravity conjecture, J. High Energy Phys. 12 (2014) 087.
- [41] B. Bellazzini, C. Cheung, and G. N. Remmen, Quantum gravity constraints from unitarity and analyticity, Phys. Rev. D **93**, 064076 (2016).
- [42] C. Cheung and G. N. Remmen, Positivity of curvaturesquared corrections in gravity, Phys. Rev. Lett. 118, 051601 (2017).
- [43] Y. Hamada, T. Noumi, and G. Shiu, Weak gravity conjecture from unitarity and causality, Phys. Rev. Lett. 123, 051601 (2019).
- [44] B. Bellazzini, M. Lewandowski, and J. Serra, Positivity of amplitudes, weak gravity conjecture, and modified gravity, Phys. Rev. Lett. 123, 251103 (2019).
- [45] W.-M. Chen, Y.-T. Huang, T. Noumi, and C. Wen, Unitarity bounds on charged/neutral state mass ratios, Phys. Rev. D **100**, 025016 (2019).
- [46] Z. Bern, D. Kosmopoulos, and A. Zhiboedov, Gravitational effective field theory islands, low-spin dominance,

- and the four-graviton amplitude, J. Phys. A **54**, 344002 (2021).
- [47] P.B. Gilkey, The spectral geometry of a Riemannian manifold, J. Diff. Geom. **10**, 601 (1975).
- [48] D. V. Vassilevich, Heat kernel expansion: User's manual, Phys. Rep. 388, 279 (2003).
- [49] A. E. M. van de Ven, Explicit counter action algorithms in higher dimensions, Nucl. Phys. B250, 593 (1985).
- [50] E. s. Fradkin and A. a. Tseytlin, Quantization and dimensional reduction: One loop results for superYang-Mills and supergravities in $D \ge 4$, Phys. Lett. **123B**, 231 (1983).
- [51] R. R. Metsaev and A. A. Tseytlin, On loop corrections to string theory effective actions, Nucl. Phys. B298, 109 (1988).
- [52] F. Bastianelli, J. M. Davila, and C. Schubert, Gravitational corrections to the Euler-Heisenberg Lagrangian, J. High Energy Phys. 03 (2009) 086.
- [53] A. Ritz and R. Delbourgo, The low-energy effective Lagrangian for photon interactions in any dimension, Int. J. Mod. Phys. A 11, 253 (1996).
- [54] D. Hoover and C. P. Burgess, Ultraviolet sensitivity in higher dimensions, J. High Energy Phys. 01 (2006) 058.
- [55] Y. Abe, T. Noumi, and K. Yoshimura, Black hole extremality in nonlinear electrodynamics: A lesson for weak gravity and Festina Lente bounds, J. High Energy Phys. 09 (2023) 024.
- [56] S. Barbosa, S. Fichet, and L. de Souza, On the black hole weak gravity conjecture and extremality in the strong-field regime, arXiv:2503.20910.
- [57] E. Palti, The swampland: Introduction and review, Fortschr. Phys. **67**, 1900037 (2019).
- [58] A. V. Manohar, Effective field theories, Lect. Notes Phys. 479, 311 (1997).
- [59] A. V. Manohar, Introduction to effective field theories, arXiv:1804.05863.
- [60] C. W. Misner, K. S. Thorne, and J. A. Wheeler, *Gravitation* (W. H. Freeman, San Francisco, 1973).
- [61] B. Zwiebach, Curvature squared terms and string theories, Phys. Lett. **156B**, 315 (1985).
- [62] W. A. Hiscock and L. D. Weems, Evolution of charged evaporating black holes, Phys. Rev. D 41, 1142 (1990).
- [63] S. Barbosa, P. Brax, S. Fichet, and L. de Souza, Running Love numbers and the effective field theory of gravity, arXiv:2501.18684.
- [64] M. Carrillo González, C. de Rham, S. Jaitly, V. Pozsgay, and A. Tokareva, Positivity-causality competition: A road to ultimate EFT consistency constraints, J. High Energy Phys. 06 (2024) 146.

- [65] G. N. Remmen and N. L. Rodd, Consistency of the standard model effective field theory, J. High Energy Phys. 12 (2019) 032.
- [66] J. A. Strathdee, Extended poincare supersymmetry, Int. J. Mod. Phys. A 02, 273 (1987).
- [67] S. Fichet and G. von Gersdorff, Anomalous gauge couplings from composite Higgs and warped extra dimensions, J. High Energy Phys. 03 (2014) 102.
- [68] I. T. Drummond and S. J. Hathrell, QED vacuum polarization in a background gravitational field and its effect on the velocity of photons, Phys. Rev. D 22, 343 (1980).
- [69] W. Heisenberg and H. Euler, Consequences of dirac theory of the positron, Zeitschr. Phys. 98, 714 (1936).
- [70] G. V. Dunne, *Heisenberg-Euler Effective Lagrangians:* Basics and Extensions (World Scientific Publishing, 2004), pp. 445–522.
- [71] S. Fichet, G. von Gersdorff, B. Lenzi, C. Royon, and M. Saimpert, Light-by-light scattering with intact protons at the LHC: From standard model to new physics, J. High Energy Phys. 02 (2015) 165.
- [72] N. Birrell and P. Davies, Quantum Fields in Curved Space, Cambridge Monographs on Mathematical Physics (Cambridge University Press, Cambridge, England, 1984).
- [73] B. Grinstein, D. Stone, A. Stergiou, and M. Zhong, Challenge to the *a* theorem in six dimensions, Phys. Rev. Lett. **113**, 231602 (2014).
- [74] B. Grinstein, A. Stergiou, D. Stone, and M. Zhong, Two-loop renormalization of multiflavor ϕ^3 theory in six dimensions and the trace anomaly, Phys. Rev. D **92**, 045013 (2015)
- [75] J. H. Schwarz, Superstring theory, Phys. Rep. 89, 223 (1982).
- [76] J. Polchinski, String Theory. Vol. 2: Superstring Theory and Beyond, Cambridge Monographs on Mathematical Physics (Cambridge University Press, Cambridge, England, 2007).
- [77] M. de Roo and M. G. C. Eenink, The effective action for the four point functions in Abelian open superstring theory, J. High Energy Phys. 08 (2003) 036.
- [78] E. S. Fradkin and A. A. Tseytlin, Nonlinear electrodynamics from quantized strings, Phys. Lett. 163B, 123 (1985).
- [79] J. M. Davila, C. Schubert, and M. A. Trejo, Photonic processes in Born-Infeld theory, Int. J. Mod. Phys. A **29**, 1450174 (2014).
- [80] M. Born and L. Infeld, Foundations of the new field theory, Proc. R. Soc. A 144, 425 (1934).
- [81] S. Fichet, G. von Gersdorff, O. Kepka, B. Lenzi, C. Royon, and M. Saimpert, Probing new physics in diphoton production with proton tagging at the Large Hadron Collider, Phys. Rev. D 89, 114004 (2014).